



Research 3D Bioprinting—Review

3D Bioprinting: A Novel Avenue for Manufacturing Tissues and Organs

Bin Zhang^{a,b,#}, Lei Gao^{a,b,#}, Liang Ma^{a,b,*}, Yichen Luo^{a,b}, Huayong Yang^{a,b,*}, Zhanfeng Cui^c

^a State Key Laboratory of Fluid Power & Mechatronic Systems, Zhejiang University, Hangzhou 310058, China

^b School of Mechanical Engineering, Zhejiang University, Hangzhou 310058, China

^c Institute of Biomedical Engineering, Department of Engineering Science, University of Oxford, Oxford OX3 7DQ, UK



ARTICLE INFO

Article history:

Received 12 October 2018

Revised 9 January 2019

Accepted 25 March 2019

Available online 3 June 2019

Keywords:

Three-dimensional bioprinting

Solid tissues

Hollow tissues

Organs-on-chips

Tissue engineering

Drug screening

ABSTRACT

Three-dimensional (3D) bioprinting is a rapidly growing technology that has been widely used in tissue engineering, disease studies, and drug screening. It provides the unprecedented capacity of depositing various types of biomaterials, cells, and biomolecules in a layer-by-layer fashion, with precisely controlled spatial distribution. This technology is expected to address the organ-shortage issue in the future. In this review, we first introduce three categories of 3D bioprinting strategies: inkjet-based printing (IBP), extrusion-based printing (EBP), and light-based printing (LBP). Biomaterials and cells, which are normally referred to as “bioinks,” are then discussed. We also systematically describe the recent advancements of 3D bioprinting in fabricating cell-laden artificial tissues and organs with solid or hollow structures, including cartilage, bone, skin, muscle, vascular network, and so on. The development of organs-on-chips utilizing 3D bioprinting technology for drug discovery and toxicity testing is reviewed as well. Finally, the main challenges in current studies and an outlook of the future research of 3D bioprinting are discussed.

© 2019 THE AUTHORS. Published by Elsevier LTD on behalf of Chinese Academy of Engineering and Higher Education Press Limited Company. This is an open access article under the CC BY-NC-ND license (<http://creativecommons.org/licenses/by-nc-nd/4.0/>).

1. Introduction

The organ shortage is a global crisis due to a rapidly increasing demand for organ transplantation and inadequate supply of organ donors [1,2]. Less than one-third of patients on the waiting list receive transplanted organs in the United States [3], while only 1×10^4 of the 1×10^6 – 1.5×10^6 people (less than 1%) who suffer from end-stage organ failure receive organ transplants in China every year [4]. Tissue-engineering approaches, which were first introduced by Langer and Vacanti [5], have been successfully applied in both research and clinical areas, such as in constructing a synthetic bladder [6]. Despite this progress, the construction of functional artificial tissues/organs requires higher spatial complexity, better intercellular interactions, and vascularization, which cannot be achieved by traditional tissue engineering methods.

In the past decades, animal models and two-dimensional (2D) cell culture validation methods have been widely used in disease studies and drug discovery [7]. However, animal models poorly mimic the underlying mechanisms in humans and tend to lead

to ethical problems, while 2D culture methods have failed to reproduce the microenvironment and recapitulate the organ-level physiology properly [7]. Therefore, the demand for more accurate three-dimensional (3D) *in vitro* models arose and the concept of organs-on-chips was introduced [8].

3D bioprinting technology has demonstrated unprecedented capability to meet these challenges. This technology has been applied in the fabrication of artificial tissue constructs with solid [9–12] or hollow structures [13–16], and of organs-on-chips [17–20], as shown in Fig. 1 [12,14,20,21]. Through 3D bioprinting, cells, biomaterials, and bioactive molecules are positioned with precise spatial control in a layer-by-layer fashion [22]. With this technology, it is possible to engineer 3D tissue constructs with specific geometries and heterogeneities and, therefore, to mimic their *in vivo* counterparts [23] in terms of both structures and functionalities.

In this article, we review the applications of 3D bioprinting. First, we consider the most popular 3D bioprinting strategies and bioinks. Next, we described the application of 3D bioprinting technology in various areas, including fabricating solid tissues and hollow tissues, and developing organs-on-chips. Finally, we summarize the challenges in this field and provide a perspective on the future applications of this technology.

* Corresponding authors.

E-mail addresses: liangma@zju.edu.cn (L. Ma), yhy@zju.edu.cn (H. Yang).

These authors contributed equally to this work.

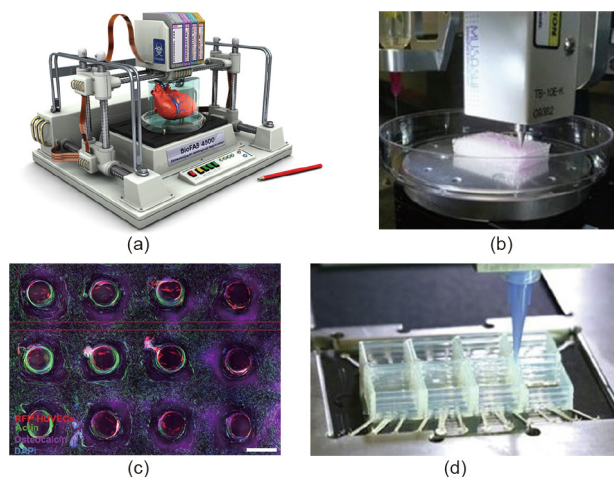


Fig. 1. Applications of 3D bioprinting technology. (a) 3D bioprinter (image courtesy of Christopher Barnett, ©2011); (b) 3D bioprinting of solid tissues; (c) 3D bioprinting of hollow tissues; (d) 3D bioprinting of organs-on-chips. (b) Reproduced from Ref. [12] with permission of Springer Nature, © 2016; (d) reproduced from Ref. [20] with permission of Springer Nature, © 2016.

2. Bioprinting strategies and bioinks

2.1. Bioprinting strategies

Inkjet-based printing (IBP) [24,25], extrusion-based printing (EBP) [10,12], and light-based printing (LBP) [16,26] are the three most commonly used bioprinting strategies [21], as shown in

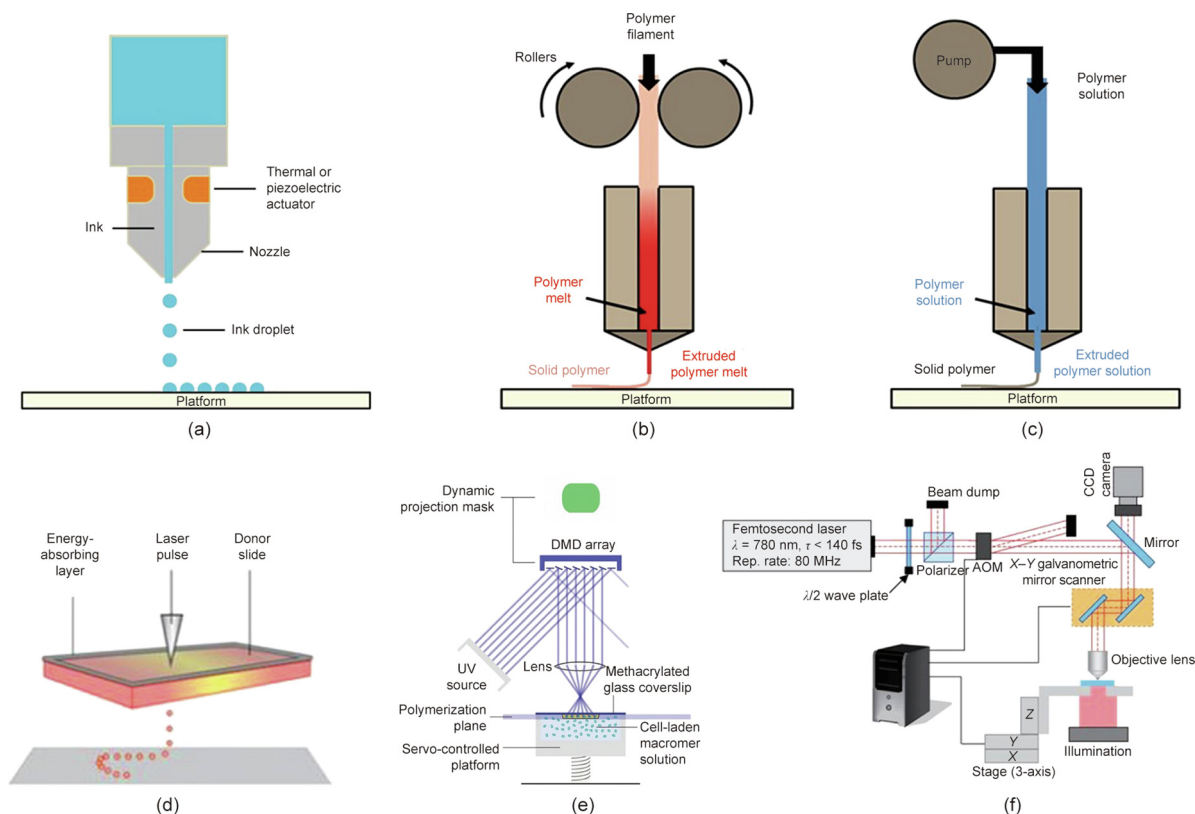


Fig. 2. Three bioprinting strategies. (a) IBP with a thermal or piezoelectric actuator; (b, c) EBP, including (b) FDM for depositing melt-cure polymers, and (c) DIW for cell-supportive hydrogels; (d–f) LBP, including (d) laser-assisted printing (LAP), (e) stereolithography (SLA), and (f) two-photon polymerization (2PP). DMD: digital micromirror device; UV: ultra violet; AOM: acousto-optic modulator. (a–c) Reproduced from Ref. [27] with permission of American Chemical Society, © 2016; (d) reproduced from Ref. [21] with permission of Springer Nature, © 2014; (e) reproduced from Ref. [28] with permission of John Wiley and Sons, © 2013; (f) reproduced from Ref. [29] with permission of Springer Nature, © 2013.

Fig. 2 [21,27–29]. Table 1 compares their advantages and disadvantages, and lists application areas of these strategies [10,12,16,18,24–26,30–33].

2.1.1. IBP

IBP, which is also known as drop-on-demand printing [34], applies thermal [35] or acoustic [34] forces to a nozzle in order to eject liquid droplets onto an electronically controlled stage (Fig. 2(a)). The first inkjet-based bioprinters were developed by modifying commercial HP inkjet printers [36,37]. One drawback of IBP is that the bioink must be in a liquid form and then cured to form a solid construct [21]. Therefore, this method can only deposit bioinks with low viscosity (3.5–12 mPa·s) and low cell density [21]. Due to the delay of curing after the droplets have been ejected, the resolution of IBP in the vertical direction (Z axis) is limited. Nevertheless, IBP is widely employed in printing skin [25], cartilage [30], bone [38,39], and blood vessels [31,40] because of its high printing speed, high throughput, high precision, and relatively low cost.

2.1.2. EBP

EBP deposits beads of paste-like biomaterials instead of liquid drops to construct tissues. Compared with IBP, EBP is more suitable for bioinks with higher viscosities [41] and higher cell densities ($> 10^8$ cells·mL⁻¹) [21]. Therefore, EBP facilitates the construction of engineered tissues with cell densities that are comparable to those of native tissues. Both melt-cure polymers and cell-supportive hydrogels can be used in EBP to construct tissues and organs [42].

Fused deposition modeling (FDM, Fig. 2(b)), which is a type of EBP, melts multiple polymers such as polycaprolactone (PCL) [12], polyurethane (PU) [43], and polylactic acid (PLA), and

Table 1

A comparison of three 3D bioprinting strategies.

Strategy	Advantages	Disadvantages	Applications	Refs.
IBP	High speed, high throughput, high precision, and low cost	Low viscosity, limited Z resolution, and low cell density	Skin Cartilage Bone	[25] [30] [24]
EBP	Suitable for high-viscosity materials, high cell density, and freeform structures	Low resolution, shear stress-induced damage	Blood vessel Blood vessel Cartilage and bone Muscle	[31] [32] [12] [10]
LBP	High resolution, complex patterns, high shape fidelity, and no viscosity limitation	Only suitable for photosensitive materials, photo-induced damage to cells, and high cost	Liver-on-a-chip Vascular networks Skin Organ-on-a-chip	[18] [16] [33] [26]

extrudes them to form prescribed geometries. Direct ink writing (DIW) (Fig. 2(c)) has the capability of depositing cell-free or cell-laden hydrogels. Researchers have extended the capability of EBP by designing coaxial nozzles [32] and developing multi-channel systems [12,43,44]. Coaxial nozzles have been widely applied in engineering microchannels [45] and vascular networks [32]. Multi-channel printing systems enable the fabrication of tissues and devices with high structural and functional complexities, such as cartilages and bones [12,46,47], muscle tissues [10,43], and a hepatic toxicity assessment platform [18]. Increasing resolution and reducing shear stress-induced damage [48] are the main challenges for developing EBP systems.

2.1.3. LBP

LBP, which includes laser-assisted printing (LAP) and stereolithography (SLA), is characterized by its superior speed among all bioprinting strategies [49], high resolution [50], and lack of limitation in material viscosity [21]. LAP, which is based on the laser-induced forward transfer (LIFT) technique, has been employed in fabricating skin-like constructs [51] (Fig. 2(d)). Koch et al. [52] carried out a parametric study to obtain optimal laser wavelength and pulse durations. SLA-approach projects light—mostly ultraviolet (UV) light—to photopolymerize hydrogels in a layer-by-layer fashion [41]. Photocrosslinkable hydrogels are selectively cured to generate specific patterns and geometries, which are determined by digital micromirror array devices (DMDs) [53]. Therefore, SLA is also known as digital light processing (DLP, Fig. 2(e)). It facilitates the construction of structures with high structural complexity, flexibility, and scalability [26,50,53]. Vascular networks with wide-range scales (50–250 μm) [16] and heterogeneous hepatic models [26] have been developed using DLP approaches. Two-photon polymerization (2PP) offers an option for fabricating 3D constructs with a submicron resolution [29,54] (Fig. 2(f)). Therefore, this technique is used to develop fine 3D structures in microfluidic devices and to replicate submicron native-like microenvironments [55,56]. However, the level of resolution of 2PP also hinders its fabrication speed and its ability to construct relatively large tissue analogues.

Recent advances in bioprinting have been focused on developing multi-nozzle bioprinters. Kang and colleagues [12] developed an integrated tissue-organ printer (ITOP) with a four-cartridge module and validated its feasibility by engineering mandible and calvarial bone, cartilage, and skeletal muscle. Lind and coworkers [20] utilized a bioprinter capable of patterning six functional bioinks with four individually addressable nozzles. The capability to deposit cells, cytocompatible hydrogels, mechanically strong polymers, and soluble factors sequentially or simultaneously will significantly improve the efficiency of the bioprinting process and facilitate the construction of tissues and organs with high structural heterogeneity and functional complexity. In addition, combining technologies such as electrospinning may enhance the

capability of bioprinting systems to create tissues/organs with multiple biomaterials, scales, and functions.

2.2. Bioinks

Bioinks—including printable biomaterials, cells, and other biologics—are materials used in 3D bioprinting to develop tissue constructs and organoids. Biomaterials provide appropriate microenvironments and structural supports for cell adhesion, migration, proliferation, and differentiation. Ideal biomaterials should have favorable tissue-specific properties in terms of processability, cytocompatibility, degradation characteristic, mechanical property, and affordability [21]. Cells are either embedded in biomaterials in the scaffold-based printing process [57] or directly printed in a form of cell spheroids or tissue strands in “scaffold-free” printing [15,46]. These cells undergo a self-assembling process to form functional tissues in the native-like extracellular matrix (ECM). Table 2 describes common bioinks used in 3D bioprinting [10–12,15,16,19,20,26,43,47,58–70].

2.2.1. Biomaterials

Three types of biomaterials—melt-cure polymers, hydrogels, and decellularized extracellular matrix (dECM)—are used in the 3D bioprinting of tissues and organs [42], as shown in Fig. 3 [10,12,15,16,20,43,45,59,66,67,68,71,72]. Composite materials with unique features have also been investigated.

Melt-cure polymers, which are generally mechanically robust and durable, can be used as structural support in tissue engineering. Examples of melt-cure polymers are PCL, PU, and PLA. PCL is a desirable supporting material due to its low melting point (60 $^{\circ}\text{C}$) in comparison with other melt-cure materials [19], which is beneficial in reducing temperature-induced cell damage. Based on this feature, Lee and Cho [19] developed a one-step approach for the fabrication of a liver-on-a-chip device using PCL as a housing material. Using the ITOP system, Kang et al. [12] printed PCL to provide supporting scaffolds in aural cartilage reconstruction and mandible bone regeneration, as shown in Fig. 3(a). In another study, PCL pillars were used to stabilize the 3D printed muscle analogue, and played essential roles in inducing the alignment of skeletal muscle cells [12].

Similarly, in the fabrication of a heart-on-a-chip device, another melt-cure polymer, PLA, was printed to form a cover to insulate the exposed wires and wells containing cells and culture media (Fig. 3(b)) [20].

PU is also a favorable biomaterial. As shown in Fig. 3(c), Merceron et al. [43] printed PU before printing cell-laden bioinks, in order to provide structural support and enough space for the deposition of cell-laden bioinks. In addition, Hsieh et al. [58] synthesized a class of thermoresponsive water-based degradable PU dispersion and embedded neural stem cells in it. This dispersion underwent gelation at approximately 37 $^{\circ}\text{C}$ with no crosslinker.

Table 2
Bioinks used for 3D bioprinting.

Bioink type	Advantages	Disadvantages	Bioink	Applications	Refs.
Melt-cure polymers	Mechanically robust and durable, and can serve as structural supporting scaffolds	Require high temperature or toxic solvents, low cytocompatibility	PCL	Cartilage, bone, and muscle	[12]
			PLA	Liver-on-a-chip	[19]
			PU	Heart-on-a-chip	[20]
Naturally derived hydrogels	Naturally cell-adherent and can provide native ECM-like microenvironments	Generally low mechanical strengths and difficult to modify	Collagen	Nervous tissue	[58]
				Muscle	[43]
			Collagen	Liver-on-a-chip	[19]
				Cartilage	[59]
			HA	Cartilage	[60]
			Alginate	Cartilage	[61]
				Vascular constructs	[62]
			Gelatin	Liver-on-a-chip	[19]
			Agarose	Vascular network	[15,63]
			Chitosan	Cartilage and bone	[64]
Synthetically derived hydrogels	Mechanical properties easy to manipulate and features such as temperature sensitivity and photocrosslinkability	The contradiction between bioactivity and processability		Skin	[65]
				Skin	[11]
				Muscle	[43]
			GelMA	Vascular networks, liver-on-a-chip	[16,26]
			PEG	Cartilage	[47,66]
				Vascular network	[63]
			Pluronic	Vascular network	[67]
dECM	Retain ECM components that induce tissue formation	Inferior post-printing shape fidelity	F-127	Cartilage and bone	[12]
				Muscle	[12]
			—	Muscle	[10]
Cell spheroids and tissue strands	High cell density No need for delivering medium or support materials	The process, which includes generating and loading spheroids, deposition, and construct handling is time-consuming	—	Bone	[68]
				Cartilage	[46]
				Vascular networks	[15]
				Nerve grafts	[69,70]

HA: hyaluronic acid; GelMA: methacrylated gelatin; PEG: polyethylene glycol.

The functions of the impaired neural system of zebrafish models were rescued after implanting the cell-laden PU constructs, suggesting the potential of this biomaterial in future applications of 3D bioprinting neuro tissues.

However, the printing of melt-cure polymers requires either high temperatures or toxic solvents, which makes this type of material less cytocompatible than other options. In addition, it is difficult to integrate these polymers with cell-supportive hydrogels in the printing process.

Hydrogels are polymeric substances that can absorb and retain a large amount of water content [57]. Hydrogels are classified into natively derived hydrogels and synthetically derived hydrogels. They undergo physical [73], chemical [26,63], or enzymatic crosslinking [11,43] to form gel-like structures.

Naturally derived hydrogels can provide native ECM-like microenvironments for cell activities. The most commonly used naturally derived hydrogels in 3D bioprinting are collagen, hyaluronic acid (HA), alginate, gelatin, agarose, chitosan, and fibrin. Collagen has been used in the construction of a liver-on-a-chip to encapsulate cells [19] and in the printing of spatially heterogeneous cartilage constructs at various concentrations [59] (Fig. 3(d)). In addition, HA [60] and alginate [61] are used to provide niches for chondrocytes. HA was modified by Ouyang and colleagues [71] so that dual crosslinking could be used to improve its long-term stability, as shown in Fig. 3(e). Due to its affordability and ease of use, alginate can be printed to form vascular conduits [45] (Fig. 3(f)) and is coupled with RGD to provide a mild condition for stem cell printing [74]. Gelatin remains in a gel-like state at low temperature, but can easily be liquefied as the temperature increases (at 37 °C). This feature allows gelatin to be applied in the development of a liver-on-a-chip [19]. Naturally derived hydrogels are also used to construct vascular networks with branch structures (Fig. 3(g)) [15], skin tissues [11], and muscle constructs [43]. Although naturally derived hydrogels have been

widely applied in various tissue-engineering areas, their low mechanical strength is still their main limitation.

In comparison with naturally derived hydrogels, synthetically derived hydrogels can be more easily modified to improve their mechanical properties and cell-adherent characteristics. Methacrylated gelatin (GelMA), polyethylene glycol (PEG), and Pluronic F-127 are three examples of this category. GelMA and PEG are both photocrosslinkable with the presence of photoinitiators [57]. GelMA is widely used in LBP and EBP [75]. For example, Zhu's research group [16] utilized GelMA hydrogel to generate complex vascular networks with gradient channel width and to develop a hepatic model (Fig. 3(h)) by positioning three types of cells precisely and rapidly [26]. PEG can be used as a sacrificial material without affecting cell viability upon its removal [66], as shown in Fig. 3(i). PEG-based hydrogels, such as polyethylene glycol diacrylate (PEGDA), poly(ethylene glycol) methacrylate (PEGMA), and poly(ethylene glycol)-tetra-acrylate (PEGTA), have been developed for cartilage and bone engineering [47,76], and for the construction of a vascular network [63]. Pluronic F-127 is temperature-sensitive, and undergoes liquefaction at low temperatures. It has been used as a sacrificial material for cartilage, bone, and muscle engineering [12], as well as in constructing perfusable endothelialized vascular channels [67] (Figs. 3(j, k)).

The main issue of hydrogel-based bioprinting is the contradiction between bioactivity and processability. Higher concentration and crosslinking density normally result in better printability and shape fidelity [77]. However, they also lead to smaller pore size and lower cell viability. Therefore, hydrogels of low concentration are used as cell-encapsulation materials [63,78] for bioprinting. Yin et al. [77] developed a novel two-step method for printing the composite of low-concentration GelMA (5%) and gelatin (8%), and achieved similar processability as high-concentration GelMA (30%) with much better cell compatibility. This is a potential strategy for printing hydrogels with both fine printability and cytocompatibility.

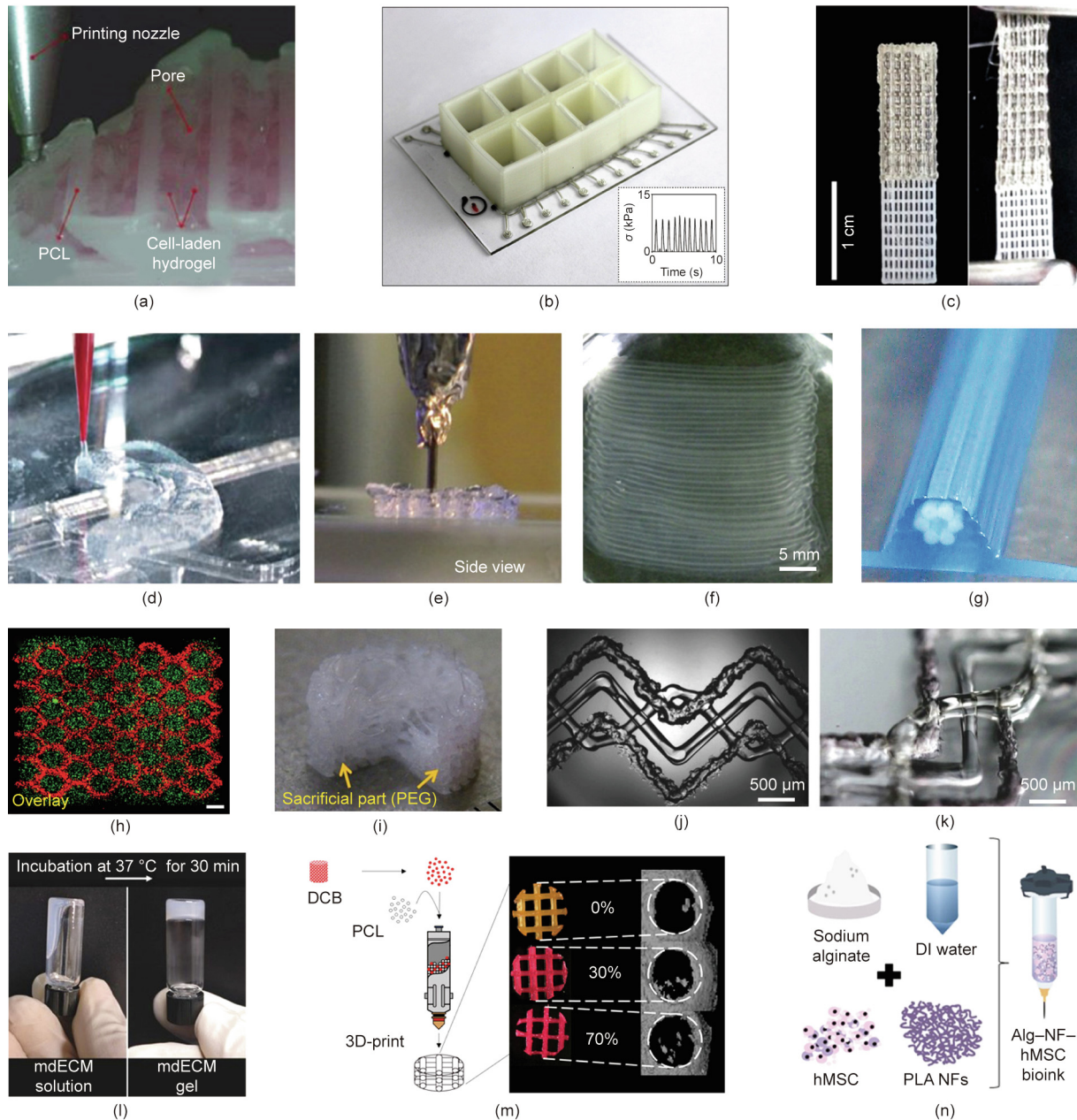


Fig. 3. Biomaterials used in 3D bioprinting. (a–c) Melt-cure polymers: (a) PCL used as structural support material of cell-laden hydrogels for mandible bone reconstruction; (b) covers printed from PLA for insulating exposed wires and cell-containing wells; (c) PU scaffolds provide pores and space which are then filled by cell-laden bioinks. (d–g) Naturally derived hydrogels: (d) high-density collagen hydrogels used for cartilage tissue engineering; (e) printing process of a dual-crosslinked HA hydrogel; (f) vascular conduits constructed by the coaxial printing of alginate hydrogels and calcium chloride solution; (g) an agarose mold for cell spheroids fusion and self-assembly for the formation of vascular structures. (h–l) Synthetically derived hydrogels: (h) fluorescent image of a GelMA-based hydrogel construct laden with hiPSC-derived hepatic cells and supporting cells; (i) PEG as sacrificial materials for fabricating complex hydrogel structures for ear regeneration; (j, k) evacuating liquefied Pluronic F-127 to generate perfusable channels. (l, m) dECM: (l) gelation process of decellularized skeletal muscle bioink, mdECM: decellularized skeletal muscle extracellular matrix; (m) a blend bioink consisting of decellularized bone (DCB) ECM and PCL used for bone regeneration. (n) Composite material: one example is the addition of PLA nanofibers (NF) into cell-laden alginate hydrogels (Alg) to promote cell proliferation and chondrogenic differentiation of human mesenchymal stem cells (hMSCs). DI: deionized. (a) Reproduced from Ref. [12] with permission of American Chemical Society, © 2016; (b) reproduced from Ref. [20] with permission of Springer Nature, © 2016; (c) reproduced from Ref. [43] with permission of IOP Publishing, © 2015; (d) reproduced from Ref. [59] with permission of American Chemical Society, © 2016; (e) reproduced from Ref. [71] with permission of American Chemical Society, © 2016; (f) reproduced from Ref. [45] with permission of Elsevier, © 2015; (g) reproduced from Ref. [15] with permission of Elsevier, © 2009; (h) reproduced from Ref. [16] with permission of Elsevier, © 2017; (i) reproduced from Ref. [66] with permission of IOP Publishing, © 2009; (j, k) reproduced from Ref. [67] with permission of John Wiley and Sons, © 2014; (l) reproduced from Ref. [10] with permission of John Wiley and Sons, © 2016; (m) reproduced from Ref. [68] with permission of American Chemical Society, © 2016; (n) reproduced from Ref. [72] with permission of American Chemical Society, © 2016.

The dECM overcomes the aforementioned drawback since it retains ECM components [57]. Perniconi et al. [79] demonstrated that acellular scaffolds explanted from mice supported the formation of myofibers, which suggests that dECM could provide suitable niches in this process. Pati's group [80] developed adipose-,

cartilage- and heart tissue-dECM bioinks and verified the feasibility of these tissue-specific dECM materials in 3D bioprinting. Functional skeletal muscle constructs were fabricated using skeletal-derived dECM bioink (Fig. 3(l)), which provided a myogenic microenvironment [10]. Moreover, the notable upregulation

of the osteogenic genes of human adipose-derived stem cells in dECM-PCL scaffolds (Fig. 3(m)), compared with that in PCL scaffolds, suggests the effectivity of decellularized ECM material in bone regeneration [68]. However, the inferior post-printing shape fidelity must be addressed in future. In addition, dECM may result in ethical issues when translated from laboratory to clinical settings, due to its origin.

Composite materials combine the advantages of each component, and potentially improve the properties of the components in terms of mechanical strength, printability, biocompatibility, and gelation characteristic. For example, by introducing various nanofibers into hydrogels, the hydrogel's mechanical property can be improved significantly and its cellular activities can be enhanced. Dolati et al. [13] reported that the addition of carbon nanotubes reinforced the strength of alginate-based vascular conduits. A bioink composed of nanofibrillated cellulose and alginate not only exhibited fine shape fidelity, but also supported the proliferation and redifferentiation of human nasal chondrocytes (hNCs) for auricular cartilage reconstruction [61]. Higher levels of cell proliferation and metabolic activity were observed in PLA-nanofiber-reinforced bioink, as shown in Fig. 3(n), and chondrogenic differentiation was exhibited [72]. These microenvironmental cues at multiple scales are believed to control the behavior of cells by means of the contact guidance of nanofibers and the tailored permeability of the hydrogel matrix [81].

The gelation characteristics can be regulated by blending various biomaterials. A visible-light-curable material was achieved by mixing PEGDA and GelMA hydrogel with eosin Y-based photoinitiator [82]. Modified HA, which underwent dual crosslinking, demonstrated better long-term stability than guest-host assembly or photopolymerization alone [71]. Alginate–GelMA-based bioinks, which also underwent dual-step gelation, were used in the bioprinting of perfusable vascular constructs and a heart-on-a-chip device [32,83]. Furthermore, by introducing nanomaterials such as gold nanoparticles or carbon nanotubes into bioinks, electroactive tissues can be developed [84] and their conductivity is manipulated.

In addition, post-printing modification, including architectural reconfiguration and surface functionalization, has been implemented to enhance the capability of 3D bioprinting and improve the bio-functionality of engineered biomaterials [85].

2.2.2. Cell spheroids and tissue strands

The formation of tissues/organs requires appropriate intercellular signaling and autonomous organization so that physiological structures can be developed [21]. When used as bioinks (Fig. 4), cell spheroids and tissue strands make it possible to mimic the developing processes of native tissues and organs. Jakab et al. [86] verified the feasibility of using spherical cell aggregates as bioinks by means of both experimental and simulation studies. The time evolution of cell spheroid patterns is shown in Fig. 4(a). The fusion can be observed after long-term incubation. Fig. 4(b) shows a structure that was constructed by depositing cell spheroids onto agarose rod molds in a study conducted by Norotte and colleagues [15]; this structure was shown to facilitate the construction of single- and double-layered vascular conduits. In a recent study, Yu et al. [46] produced “tissue strands” by microinjecting cells into alginate capsules (Figs. 4(c, d)). After cell aggregation, scaffold-free tissue strands could be directly printed on the “bio-paper” with no delivering medium or supporting structure.

Since cell spheroids and tissues strands are generated by directly assembling cells, high cell density can be achieved using these two types of materials. High cell density is vital when developing artificial tissues such as myocardial tissues and vessels [15]. Therefore, these bioinks may play important roles in developing long-life functional tissues with dense vascular networks.

2.2.3. Cell sources

The cell sources currently used in 3D bioprinting are either various types of primary cells or stem cells. By depositing multiple primary cell types in predetermined patterns, printed constructs can mimic the functions of their *in vivo* counterparts. However, the finite lifespan of many types of primary cells limits the long-term functioning of engineered constructs post-transplantation

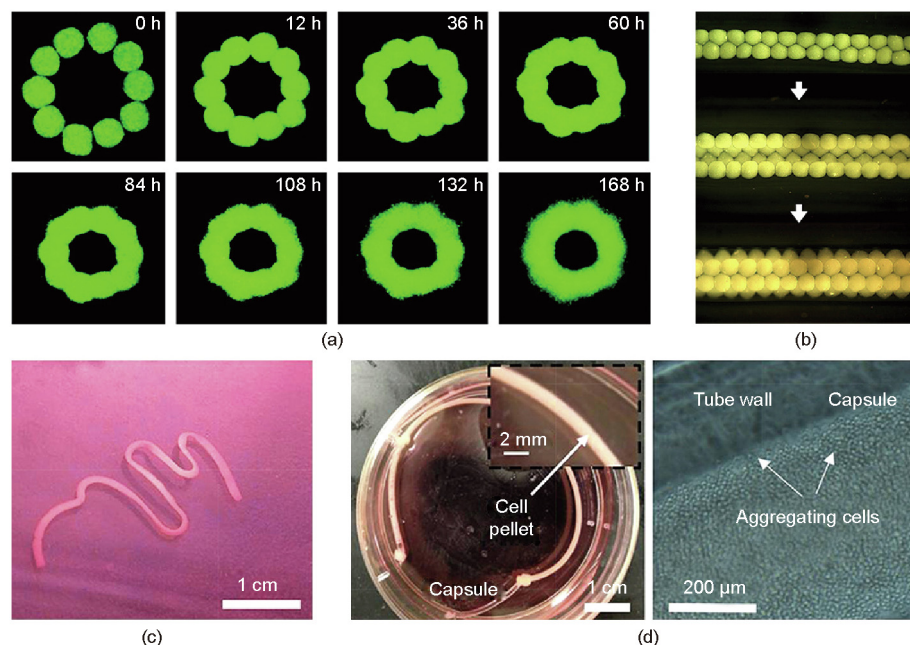


Fig. 4. Cell spheroids and tissue strands as bioinks. (a, b) Cell spheroids: (a) Time evolution of patterns of cell spheroids; (b) cell spheroids fused into tubular and branched structures. (c, d) Tissue strands: (c) An 8 cm long tissue strand; (d) aggregating cell pellet supported by alginate capsules. (a) Reproduced from Ref. [86] with permission of National Academy of Sciences, © 2004; (b) reproduced from Ref. [15] with permission of Elsevier, © 2009; (c, d) reproduced from Ref. [46] with permission of Springer Nature, © 2016.

[21]. Therefore, the stem cell is a promising option due to its longevity, self-renewal, and pluripotency/multipotency [21].

Embryonic stem cells (ESCs) and induced pluripotent stem cells (iPSCs) have the capability of differentiating into any cell type and have long-term proliferative potential [87]. The differentiation of stem cells is mainly influenced by biological, chemical, and physical cues [88]. Although studies have been carried out to regulate cellular microenvironments by depositing growth factors with defined spatial gradients [89], the underlying mechanisms of stem cell differentiation need to be further investigated and better understood. In addition to engineering appropriate microenvironments for stem cells, the printing process is required to provide suitable physical cues, such as shear stress, while maintaining high viability and the pluripotency of stem cells. For example, Ouyang et al. [90] systematically investigated the effects of 3D bioprinting parameters on stem cell viability, proliferation, and maintenance of pluripotency. Upon parameter optimization, they successfully engineered ESCs-laden constructs with a viability of 90%, and the ESCs remained in an undifferentiated state after printing. One challenge of printing ESCs and iPSCs is the risk of tumorigenicity [91]; ethical issues should also be taken into consideration [88]. Adult stem cells (ASCs) are undifferentiated stem cells that are capable of self-renewal. These can be derived from various sources such as bone marrow, adipose tissues, and liver [92]. Mesenchymal stem cells (MSCs, one type of ASC) derived from bone marrow [93] and adipose tissues [94] have been used in bioprinting artificial tissues/

organs [76,95]. MSCs are believed to be less tumorigenic [91] and thus safer than ESCs and iPSCs.

Although stem cell printing is still in its infancy, the combination of 3D bioprinting technology and stem cell technology has shown promise for engineering tissues and organs. Moreover, it is possible that this combination could be used to develop patient-specific disease models and drug-testing platforms.

3. Solid tissues

Solid tissues are defined as tissues without hollow structures inside. Researchers have 3D bioprinted solid tissues for tissue regeneration. Cartilage [24,59,96,97], bone [38,39,68,98], skin [11,99], and muscle [10,20,43] are discussed in this section.

3.1. Cartilage and bone

Cartilage and bone are the tissues with the highest mechanical strengths in human bodies. Studies on cartilage and bone have recently focused on improving mechanical properties and achieving patient-specific geometries [100]. In addition, the osteochondral interface and the interface between printed parts and native tissues play crucial roles in repairing osteochondral defects [101].

Cartilages are elastic connecting tissues that constitute major parts of ears, noses, and joints (Fig. 5(a–c)). Articular cartilages draw the most interest due to their complex layered structure

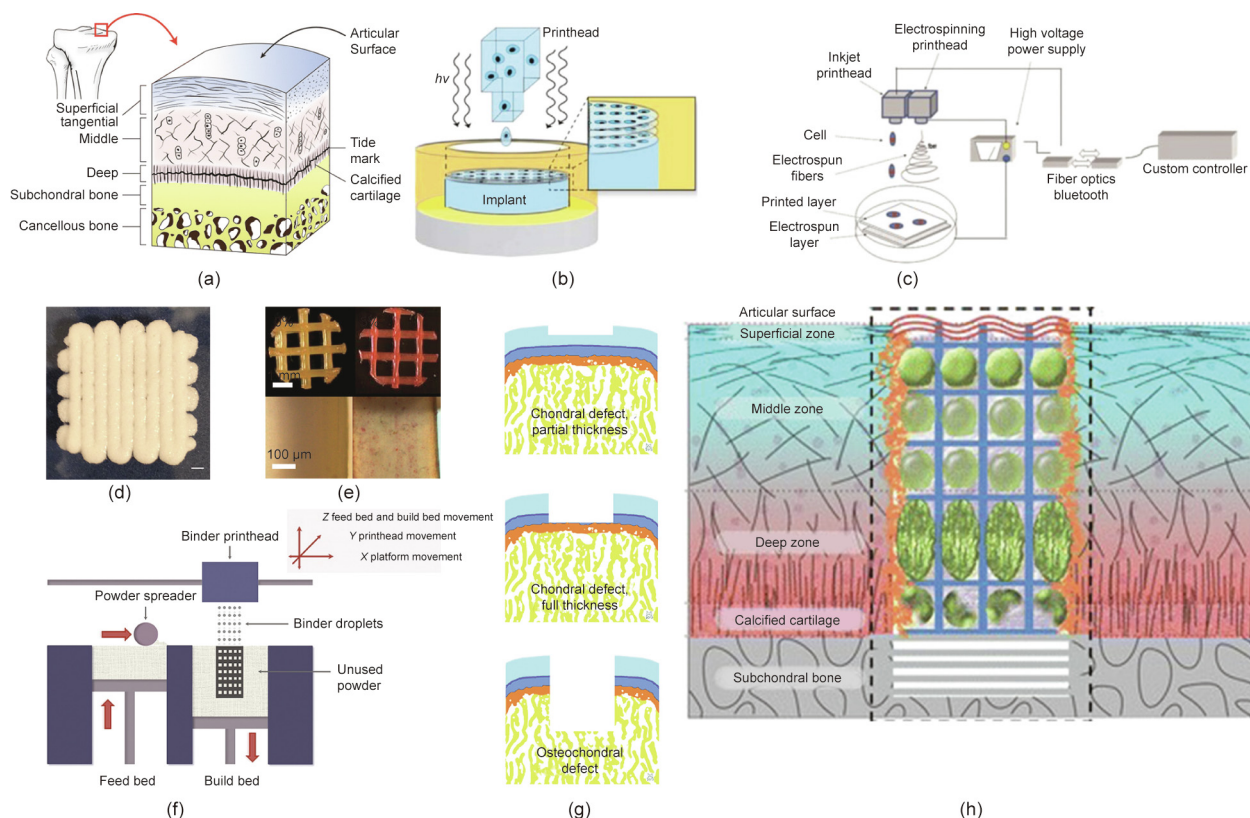


Fig. 5. 3D bioprinting of cartilages and bones. (a–c) 3D bioprinting of cartilage: (a) Layered structure of cartilage; (b) inkjet printing cartilage plugs using acrylated PEG hydrogel with simultaneous photopolymerization; (c) a hybrid printing approach that combines IBP and electrospinning. (d–f) 3D bioprinting of bone: (d) Printed bone constructs with equivalent mechanical properties to those of human cancellous bone; (e) human adipose-derived stem cells (hASCs) cultured in DCB-PCL scaffolds exhibited notable upregulation of osteogenic genes and osteogenesis; (f) bone constructs constructed by jetting binder droplets on powder materials. (g, h) Osteochondral interface construction: (g) Osteochondral defects with different thickness, including the partial chondral defect, full thickness chondral defect, and osteochondral defect [103]; (h) modular tissue assembly strategy for repairing osteochondral defect [107]. (a) Reproduced from Ref. [102] with permission of Springer Nature, © 2014; (b) reproduced from Ref. [24] with permission of John Wiley and Sons, © 2015; (c) reproduced from Ref. [96] with permission of IOP Publishing, © 2016; (d) reproduced from Ref. [98] with permission of IOP Publishing, © 2009; (e) reproduced from Ref. [68] with permission of American Chemical Society, © 2016; (f) reproduced from Ref. [39] with permission of Elsevier, © 2016; (g) reproduced from Ref. [103] with permission of Mary Ann Liebert, Inc., © 2014; (h) reproduced from Ref. [107] with permission of Springer Nature, © 2016.

(Fig. 5(a)), from the articular surface to calcified cartilage in depth [102]. These layers are involved in different osteochondral defects: partial chondral defect, full chondral defect, and osteochondral defect [103]. The IBP strategy has been employed for direct cartilage repair with simultaneous UV polymerization [24,30] (Fig. 5(b)). An electrospinning system was then integrated with the IBP system (Fig. 5(c)) to produce mechanically stronger tissue constructs [96]. The development of printed cartilage tissues can be significantly affected by the properties of bioinks. It has been reported that alginate and agarose hydrogels support the development of hyaline-like cartilage, while GelMA and a PEGMA-based hydrogel supported the development of a more fibrocartilage-like tissue [47]. Nanofibrillated cellulose [61,97,104] and PLA nanofibers [72] have been combined with cell-laden alginate hydrogel to improve cell density and reinforce the mechanical strength. High-density collagen was found to be a preferable material in load-bearing applications of artificial cartilages due to its mechanical stability and capability of maintaining cell growth [59].

Studies on 3D bioprinting for bone regeneration and repair have been carried out using both EBP and IBP (Figs. 5(d–f)). Sawkins and colleagues [98] printed PLGA-based constructs that had yield stresses and Young's modulus within the range of the properties of human cancellous bone (Fig. 5(d)). Apart from high mechanical strength, angiogenesis and osteogenesis are crucial in the fabrication of functional bone implants. With decellularized bone (DCB) matrix and PCL as bioinks (Fig. 5(e)), human adipose-derived stem cells exhibited significant upregulation of osteogenic genes [68]. Lv and colleagues [105] incorporated the controlled release of vascular endothelial growth factors (VEGFs) with 3D bioprinting to improve osteogenesis and angiogenesis. The IBP strategy was used to deposit binder droplets onto powders (Fig. 5(f)), such as hydroxyapatite (HA) and tricalcium phosphate (TCP), to fabricate bone-like constructs [38,39].

Constructing the osteochondral interface (Figs. 5(g, h)) is the most challenging part of engineering osteochondral implants [106], especially for a full-thickness osteochondral defect from the articular joint surface to subchondral bone (Fig. 5(g)). A modular assembly strategy (Fig. 5(h)) for osteochondral lesion repair was proposed by Schon and colleagues [107]. 3D bioprinting has shown promise in this field due to its capability of precisely depositing various materials into multilayer gradient constructs. Simultaneous UV photopolymerization of acrylated PEG hydrogel noticeably enhanced the osteogenic and chondrogenic differentiation [24].

In summary, further studies should be carried out to engineer osteochondral constructs with gradient structure [108] and better mechanical performance. Gradient structures can potentially integrate with both soft chondral and the hard subchondral host environment. Suitable microenvironments should be constructed to improve cell proliferation and differentiation. Growth factors and their controlled release should be integrated into the printing process to improve the functionality of engineered constructs.

3.2. Skin

Skin is the largest organ in the human body, and plays a significant role in the immune system as the first defense barrier [109]. Scratches, burns, diabetic foot ulcers, and dermatonecrosis are the main causes of skin defects, which require a large number of skin substitutes for treatments. As cosmetic product testing on animals is forbidden in most countries, functional artificial skins are urgently required in the cosmetic industry [110].

The basis of functional skin models is a double-layer structure with both dermis and epidermis. Inkjet-based 3D freeform fabrication (FF) was first implemented to print both fibroblasts and keratinocytes with collagen to form dermal/epidermal-like distinctive layers in a hydrogel scaffold [111] (Fig. 6(a)). In a similar

experiment, a multi-layered skin model was constructed and cultured at the air–liquid interface [112]. The printed skin tissue demonstrated better shape fidelity, compared with the manual-deposition model, and exhibited distinct layers of the epidermis and dermis (Fig. 6(c)). To overcome the difficulty of fabricating well-shaped 3D scaffold structures with collagen or alginate, a novel cryogenic plotting system was developed by Kim and colleagues [113], as shown in Fig. 6(b). The collagen solution was laid down layer by layer at -40°C and then placed in a freeze-dryer at -76°C for 3 d. The structure, which had a porosity of 98%, showed good performance with co-cultured keratinocytes and fibroblasts. The same group then designed a hybrid (core/shell) scaffold composed of outer collagen and inner alginate to improve the mechanical stability of these skin scaffolds [114] (Fig. 6(d)). The Young's modulus of these hybrid scaffolds increased by approximately seven times compared with pure collagen scaffolds, while the biocompatibility was at a similar level, according to *in vitro* and *in vivo* tests (Fig. 6(e)). Amniotic fluid-derived stem (AFS) cells and bone marrow-derived MSCs were re-suspended in the fibrin-collagen gel and printed over the wound site of nude mice by means of an IBP strategy [25] (Fig. 6(f)). The healing rate increased in comparison with the control group. Kim and colleagues [115] engineered a skin model by combining EBP and IBP strategies. A human skin model was fabricated with a functional transwell system in a single-step process, at 50 times lower cost and ten times less medium than a conventional culture (Fig. 6(g)).

Besides EBP and IBP, the LAP approach has been employed to print cell-level-resolution skin [51]. NIH-3T3 fibroblasts and human keratinocytes embedded in collagen gel served as bioink and were printed onto a sheet of MatrigelTM; the paralleled layers demonstrated the micropatterning capabilities of LAP (Fig. 6(h)). Dorsal skinfold chambers in nude mice were employed to evaluate further functions of the artificial tissue [33] (Fig. 6(i)). New vessels were found in the wound area of the mice.

Thus far, most skin printing studies have focused on the geometrical structure of the epidermis and dermis. However, the vascularization of skin substitutes is of great significance for clinical applications. 3D bioprinting technology combined with tissue engineering using iPSC-derived cells was employed to investigate the vascularization of engineered human skin constructs [99] (Fig. 6(j)). Micropatterned vascular networks were established, and demonstrated the capabilities of promoting and guiding neovascularization during the healing period. Endothelial progenitor cells and adipose-derived stem cells, which were embedded in engineered skin substitutes, were found to accelerate the neovascularization *in vivo* [116]. Further investigation of the vascularization of skins, as well as the involvement of secondary and adnexal structures, should be performed. Recently, studies have been carried out to develop pigmented skin constructs with melanocytes printed precisely in the dermis-epidermis junction [117,118]. These results imply that completely functional skin substitutes can be engineered by 3D bioprinting technology.

3.3. Muscle

The printing of muscles has drawn much research interest due to its potential in the treatment of muscular diseases and injuries, as well as in drug studies, as summarized in Fig. 7 [10,12,20,43,83,119].

Contractility and myogenesis are the basis of constructing functional muscles. A novel bioink based on decellularized skeletal muscle extracellular matrix (mdECM) was prepared by Choi et al. [10], and provided an appropriate myogenic microenvironment for cell proliferation, myotube formation, and myogenic differentiation (Fig. 7(a)). Merceron and colleagues [43] printed a muscle-tendon unit with an elastic PU-myoblasts muscle end and a stiff

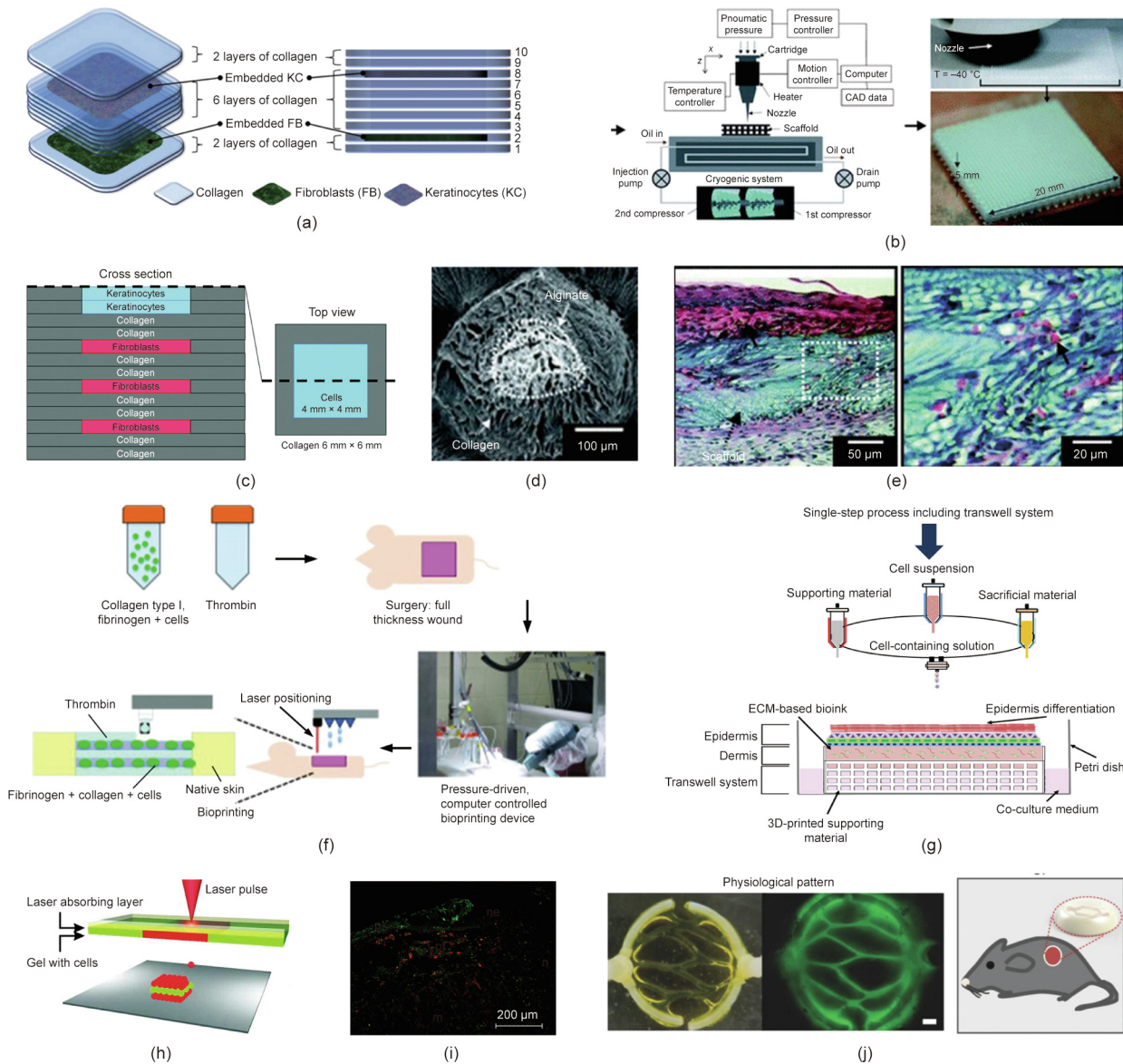


Fig. 6. 3D bioprinting of skin. (a–e) EBP for skin reconstruction: (a) Schematic of layer-by-layer printing of multi-layered skin cells and collagen; (b) schematic diagram of the cryogenic plotting system and the fabrication procedure for 3D scaffolds; (c) construction of a 3D skin tissue; (d) surface scanning electron micrograph (SEM) of the core/shell skin scaffold; (e) histological photomicrographs of transplanted areas treated with the scaffold, with the generated vasculature indicated by arrowheads. (f, g) IBP for skin reconstruction: (f) Schematic diagram of the healing approach; (g) schematic diagram describing a tissue-engineering strategy combined EBP and IBP. (h–j) LBP for skin reconstruction: (h) Sketch of the laser printing setup and its fluorography of multilayer structure; (i) tissue-engineered skin construct inserted into the wound of a nude mouse; (j) schematic description of the skin fabricating process and the development of vascularized models. (a) Reproduced from Ref. [111] with permission of Elsevier, © 2009; (b) reproduced from Ref. [113] with permission of Royal Society of Chemistry, © 1991; (c) reproduced from Ref. [112] with permission of Mary Ann Liebert, Inc., © 2014; (d, e) reproduced from Ref. [114] with permission of Royal Society of Chemistry, © 1991; (f) reproduced from Ref. [25] with permission of John Wiley and Sons, © 2012; (g) reproduced from Ref. [115] with permission of IOP Publishing, © 2009; (h) reproduced from Ref. [51] with permission of John Wiley and Sons, © 2012; (i) reproduced from Ref. [33]; (j) reproduced from Ref. [99] with permission of John Wiley and Sons, © 2016.

PCL-fibroblasts tendon end (Fig. 7(b)). High viability of cells (> 80%) was exhibited at 7 d after printing. These results suggest the possibility of printing muscles with acceptable elasticity and strength. The features of engineered muscle tissues have inspired studies on biomimetic cellular machines and micromotors [120]. Cvetkovic and colleagues [119] developed a muscle-powered biological machine (Fig. 7(d)). By applying electrical stimulation, the contraction of myocytes was triggered.

Functional muscle constructs can be used in the treatment of injury and in developing organ-on-a-chips for toxicity assessment. Kang et al. [12] fabricated a skeletal muscle construct (Fig. 7(c)) and implanted it subcutaneously with common peroneal nerves inserted. Organized muscle fibers and an innervating capability

were demonstrated when the muscle construct was harvested after two weeks of implantation.

The engineering of cardiac tissues is believed to be a promising approach for treating myocardial infarction (MI, also known as heart attack) [121]. Many efforts have been made to construct contractile and functional cardiac patches via 3D bioprinting [122,123]. Zhang and colleagues [83] investigated the vascularization of cardiac tissues by seeding cardiomyocytes into endothelialized hydrogel scaffolds (Fig. 7(e)). Embedding the organoid into a perfusion microfluidic bioreactor enabled the platform to model cardiovascular disease and evaluate cardiovascular toxicity. Lind et al. [20] developed a heart-on-a-chip (Fig. 7(f)) by integrating soft strain gauge sensors with printed laminar cardiac tissues, and

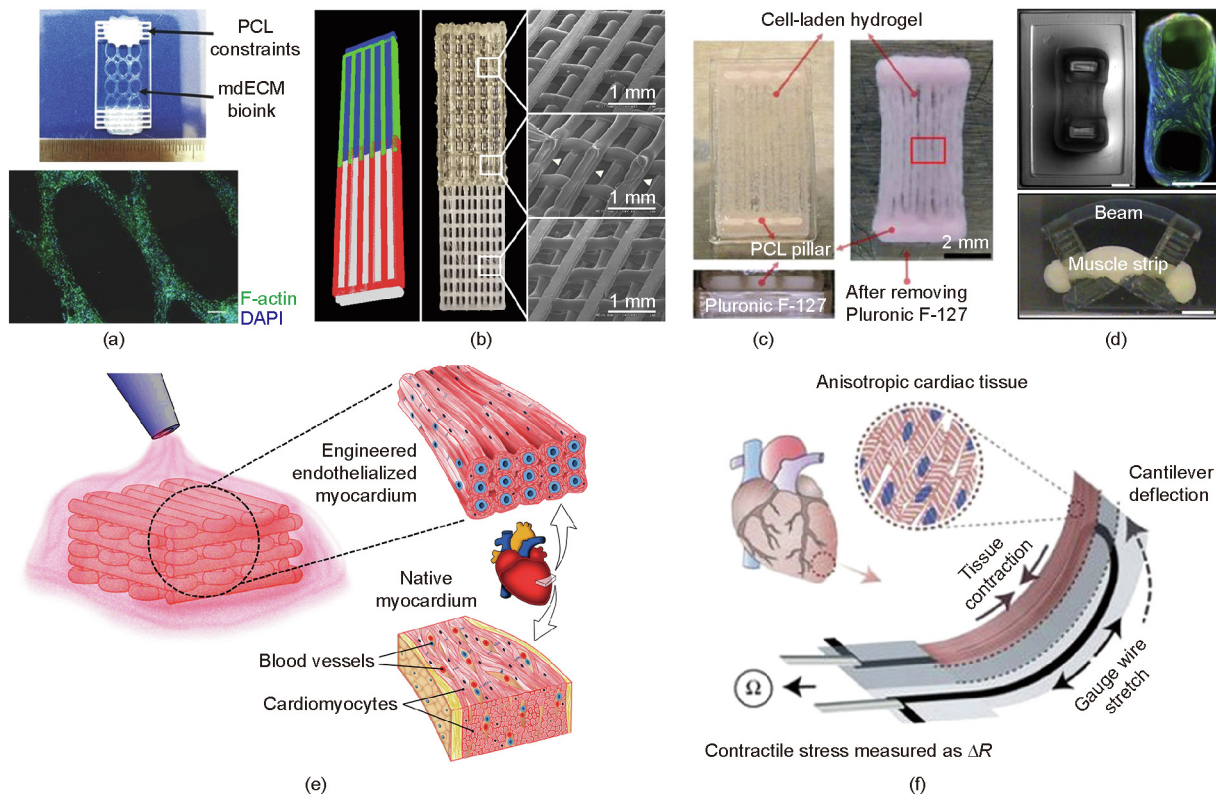


Fig. 7. 3D bioprinting of muscular tissues. (a–d) 3D bioprinting of skeletal muscles: (a) dECM is used to provide an appropriate microenvironmental niche and complex cues for promoting myogenesis and myotube formation; (b) a region-specific muscle–tendon structure was constructed using an integrated organ printing (IOP) system; (c) skeletal muscle reconstruction using PCL support, sacrificial Pluronic F-127, and cell-laden hydrogels; (d) a cellular machine (bio-bot) powered by contractile engineered muscle strip [119]. (e, f) 3D bioprinting of cardiac muscles: (e) An endothelialized hydrogel scaffold seeded with cardiomyocytes for developing a cardiovascular toxicity evaluation platform; (f) the principle of a cardiac microphysiological device (heart-on-a-chip) with integrated soft strain gauge sensors. (a) Reproduced from Ref. [10] with permission of John Wiley and Sons, © 2016; (b) reproduced from Ref. [43] with permission of IOP Publishing, © 2009; (c) reproduced from Ref. [12] with permission of Springer Nature, © 2016; (e) reproduced from Ref. [83] with permission of Elsevier, © 2016; (f) reproduced from Ref. [20] with permission of Springer Nature, ©2016.

observed tissue contraction. They investigated the response of the constructs to two drugs, and studied the contractile development in long-term culture.

4. Hollow tissues

3D bioprinting of hollow tissues is different from that of solid tissues due to the higher structural complexity. Vasculatures are hollow tissues that are mostly studied in the field of 3D bioprinting. The length scale of vasculature ranges from microscale vessels (capillaries) to millimeter-sized vessels (e.g., arteries and veins) [48]. Vasculatures of various length scales and geometric complexities require different bioprinting strategies, which are categorized into self-assembly, the perfusion-based approach, and the extrusion-based approach, as shown in Fig. 8. Table 3 lists the advantages and disadvantages of these strategies [13,15,31,35,45,62,67,69,124–129]. Other tissues with hollow structures, such as heart valves and nervous grafts, are also considered in this section.

4.1. Self-assembly

The self-assembly strategy was first proposed by Jakab et al. [86], and was then employed in tissue and organ fabrication (Fig. 8(a)). This process uses cell spheroids as bioinks or building blocks in a scaffold-free manner. After fusing into specific geometries, these spherical cell aggregates form functional tissues [130].

Norotte and colleagues [15] proposed a scaffold-free approach for the construction of double-layer vessel tubes (Fig. 8(b)). Several

cell types, including smooth muscle cells and fibroblasts, were aggregated into either cellular spheroids or cylindrical strands with controlled diameters. Cell aggregates were then deposited into molds that were constructed from agarose strands and then assembled to form blood vessels. Distinct geometries and the hierarchical tree were fabricated from carefully designed patterns of agarose strands and cell spheroids (Fig. 8(c)). Since it uses cell aggregates as bioinks, this approach can achieve the highest cell density among all bioprinting strategies. In addition, Kucukgul et al. [131,124] combined the self-assembly of cell aggregates with imaging techniques and computational algorithms to mimic a human aorta. Unlike Norotte's method, large-diameter aortas (ranging from 4 to 10 mm) were formed in the vertical direction.

However, due to the limitation of the cell spheroid sizes, the vascular walls constructed by means of the self-assembly approach were generally too thick (300–500 μm) for the diffusion of nutrients and oxygen, which requires a thickness of 100–200 μm [132]. Furthermore, the preparation time of the cell spheroids is usually time-consuming, which restricts the construction of vascular networks to scale-up tissues and organs.

4.2. Perfusion-based approach

The perfusion-based approach for the construction of vasculature is based on cell-laden hydrogel scaffolds and the perfusion of growth factors, endothelial cells, and so forth.

Neiman and colleagues [126] developed a perfusable culture system with hepatic cell-laden constructs and epidermal growth factor (EGF) perfusion to prolong the maintenance of albumin

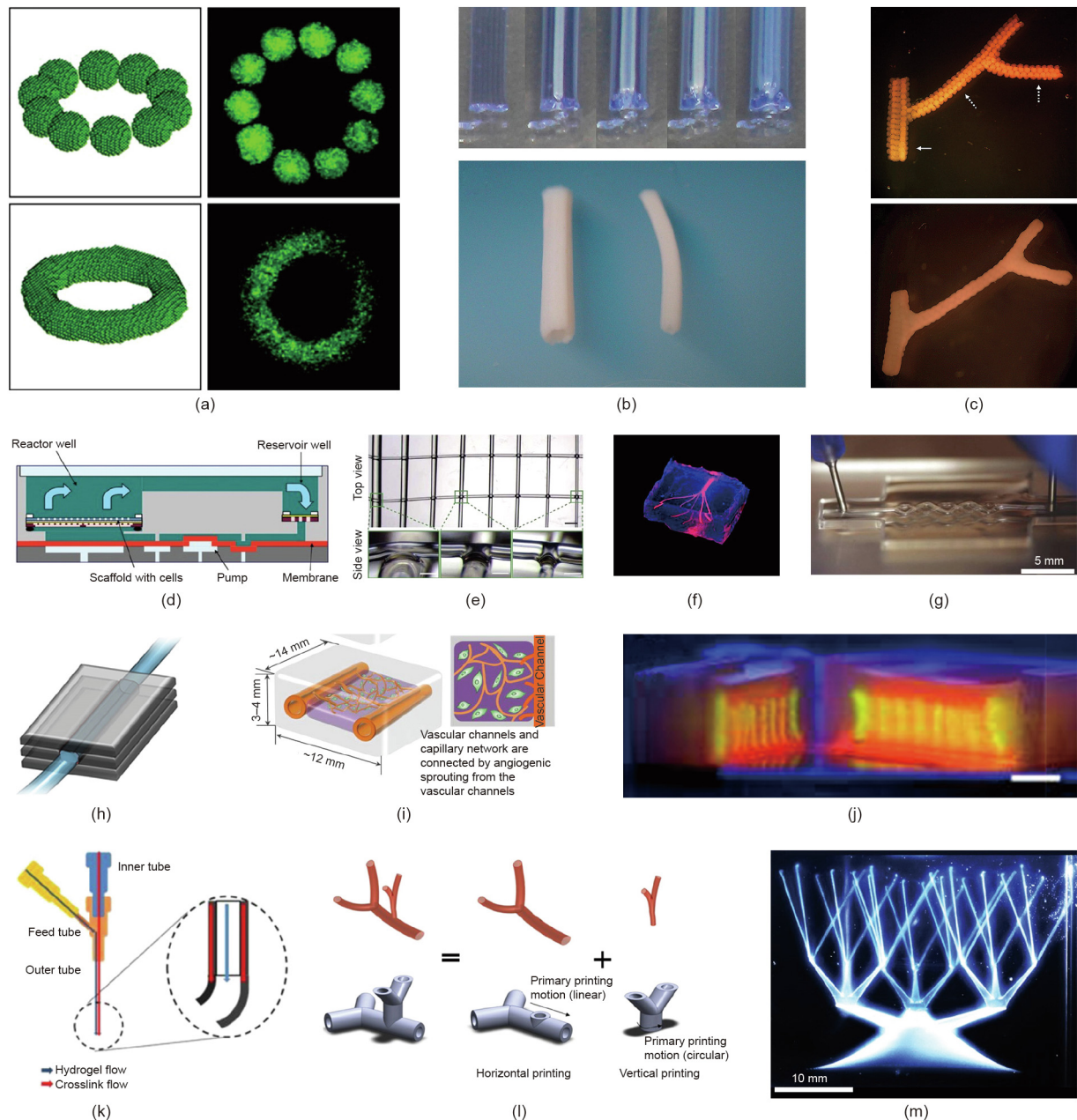


Fig. 8. 3D bioprinting of hollow tissues. (a–c) Self-assembly method: (a) Cell spheroids fuse to form tissue; (b) scaffold-free approach for the construction of vasculatures; (c) hierarchical tree by cell spheroids fusion. (d–j) Perfusion-based method: (d) Porous hepatic construct for nutrient convection; (e–g) carbohydrate glass, agarose, and Pluronic F-127 as sacrificial materials for vascular channels formation; (h, i) angiogenesis sprouting by the perfusion of soluble factors; (j) vascularized tissue with a thickness of about 1 cm [14]. (k–m) Extrusion-based method: (k) A coaxial nozzle for producing vascular conduits; (l) freeform printing of cellular structures with bifurcations, where a calcium chloride solution was utilized as both a crosslinking agent and a support material; (m) vascular networks constructed by writing in granular gel medium. (a) Reproduced from Ref. [86] with permission of National Academy of Sciences, © 2004; (b, c) reproduced from Ref. [15] with permission of Elsevier, © 2009; (d) reproduced from Ref. [126] with permission of John Wiley and Sons, © 2015; (e) reproduced from Ref. [125] with permission of Springer Nature, © 2012; (f) reproduced from Ref. [63] with permission of Royal Society of Chemistry, © 2014; (g) reproduced from Ref. [67] with permission of John Wiley and Sons, © 2014; (h) reproduced from Ref. [31] with permission of Elsevier, © 2014; (i) reproduced from Ref. [40] with permission of Springer Nature, © 2014; (k) reproduced from Ref. [13] with permission of IOP Publishing, © 1990; (l) reproduced from Ref. [62] with permission of John Wiley and Sons, © 2015; (m) reproduced from Ref. [128].

Table 3
Comparison of strategies for vasculature construction.

Strategy	Advantages	Disadvantages	Refs.
Self-assembly	High cell density; capable of constructing the double-layered vascular wall	Vascular walls too thick due to limited resolution; formation of cell spheroids is time-consuming	[15,35,69,124]
Perfusion-based	Effects of soluble factors and fluid mechanics can be studied	Relatively low cell density	[31,67,125–127]
Extrusion-based	Capability to fabricate highly geometrically complex structures	Shear stress-induced cell damage; limited availability of biomaterials	[13,45,62,69,128,129]

production (Fig. 8(d)). However, since the constructs were tortuous, it was difficult for them to be endothelialized for vasculature formation. Besides, the absence of an inlet and outlet prevented the construct from being integrated with native vascular networks if implanted.

Various materials have been utilized as sacrificial materials to fabricate vascular networks (Figs. 8(e–g)). Miller et al. [125] patterned carbohydrate glass into a lattice geometry enveloped by agarose, alginate, PEG, and so forth to form 3D networks. After the carbohydrate glass was melted, the endothelial cell suspension was injected into the vascular-like structure. The endothelial cells adhered to the inside walls of the channel such that vasculature networks were generated. Agarose was employed to fabricate microchannels networks by Bertassoni and colleagues [63] and an endothelial monolayer was observed. Temperature-sensitive materials such as Pluronic F-127 have demonstrated capability in the construction of vascularized heterogeneous tissues [67]. For example, Suntornnond et al. [133] developed a Pluronic–GelMA-based structure and used Pluronic as a sacrificial material to fabricate a hollow quad-furcated vascular-like structure. This study suggests that 3D bioprinting can fabricate freestanding 3D vascular networks other than bulk constructs with perfusable channels, as described in other references.

Apart from the perfusion of cell suspension, studies have been carried out to investigate the effects of soluble factors on angiogenic processes. With the perfusion of angiogenic factors through channels other than endothelialized channels, endothelial sprouts and adjacent capillary networks have been formed [127,31,40], as shown in Figs. 8(h, i). These studies suggest the possibility of constructing multiscale vascular networks.

Recently, Kolesky and coworkers [14] constructed large-scale (thickness > 1 cm) vascularized tissues, which opened new avenues for the construction of human-scale tissues containing a vascular network (Fig. 8(j)).

4.3. Extrusion-based approach

The extrusion-based approach for constructing vasculatures focuses on the geometrical complexity and branching structures. Vascular conduits with 500–1000 μm diameters were produced utilizing a coaxial extrusion approach [13,45,129]. Carbon nanotubes were added into the hydrogel (Fig. 8(k)) to improve the mechanical strength [13].

The most geometrically complex vascular trees were constructed by researchers at the University of Florida. The first approach involved extruding cell-laden alginate hydrogel into a calcium chloride solution pool to form structures with horizontal and vertical bifurcations [62] (Fig. 8(l)). The second approach involved jetting cell-laden collagen into granular gel medium that could smoothly transition between the fluid and solid states under shear stresses [128]. A continuous vessel network with diameters spanning several orders of magnitudes (from 100 μm to the centimeter scale, Fig. 8(m)) was developed.

In summary, the construction of vascular networks requires increasing geometrical complexity and functionality. Uniaxial channels and vascular lattices can no longer meet the demand of the vascularization of thick tissues. 3D branching networks should be integrated into complex tissues to facilitate nutrient delivery and metabolic activities. For further application of 3D printed vasculatures, other printing strategies, such as SLA [16], can be integrated into this application area as well. Vascular networks can be applied in many areas [48]. They can provide experimental platforms for investigating the complex process of angiogenesis *in vitro*. The effects of soluble factors, such as VEGF, on tissue functions can be studied using perfusable vascularized constructs. Printed tissues with vascular networks can be used as disease

models and drug-screening platforms. Vascularization is also essential for the construction of clinically transplantable tissues and organs.

4.4. Other hollow tissues

Researchers have also carried out studies on fabricating other hollow-structure tissues, such as nerve grafts [70] and heart valves [69], as shown in Fig. 9 [134,135].

Nerve injury has severe effects on the quality of life of patients. Autologous grafts are the gold standard in nerve repairing. Owens and colleagues [70] constructed novel multi-lumina nerve grafts (Fig. 9(a)) using a scaffold-free 3D bioprinting approach that is similar to Norotte's method of fabricating blood vessels [15]. The results provided evidence that the bioprinted nerve graft was a potential option for nerve regeneration [70].

As a growing health problem, heart valve disease normally requires prosthetic replacement. Mechanical valves, bioprosthetic valves, and pulmonary autografts are current options for heart valve replacement, but are inadequate, particularly for younger patients [134]. Engineering aortic valves by 3D bioprinting is an option to address this issue. Duan and colleagues used 3D models either reconstructed from μCT images [134] or designed by Solidworks® [135] and successfully engineered heterogeneous cell-laden aortic valve hydrogel conduits, as illustrated in Figs. 9(b–d). The human aortic valvular interstitial cells (hAVICs), which were encapsulated in hydrogel-based conduits, maintained high viability and expressed certain proteins [135].

5. Organs-on-chips

Organs-on-chips combine microfluidic technology with 3D bioprinting technology to develop disease models, drug discovery platforms, and high-throughput assays. They provide a 3D extracellular environment that mimics native ECM. Therefore, cells demonstrate more realistic responses to drugs, compared with those under 2D culture conditions [136]. Studies on fabricating organs-on-chips by 3D bioprinting have been mainly focused on liver-on-a-chips and heart-on-a-chips. 3D bioprinting also has potential for developing a body-on-a-chip [137].

5.1. Liver-on-a-chip

Hepatic toxicity is one of the most important aspects of drug screening and toxicity testing. Organovo, Inc. focuses on

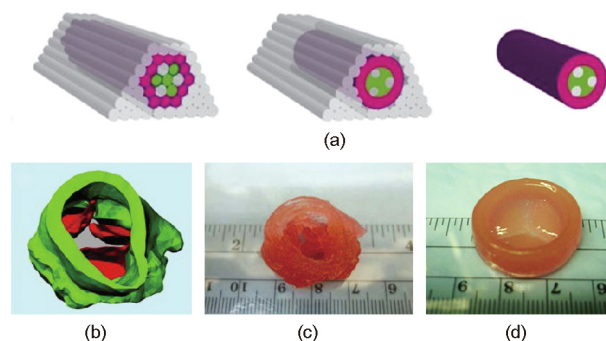


Fig. 9. Bioprinted hollow tissues. (a) Nerve graft with multiple lumina. (b–d) Heart valves: (b, c) Aortic valve model constructed from micro-computed tomography (μCT) images and as-printed aortic valve conduit; (d) aortic valve with encapsulation of human aortic valvular interstitial cells (hAVIC) within leaflets. (a) Reproduced from Ref. [70] with permission of IOP Publishing, © 2009; (b, c) reproduced from Ref. [134] with permission of John Wiley and Sons, © 2012; (d) reproduced from Ref. [135] with permission of Elsevier, © 2014.

developing liver tissue systems for drug development [138–140]. A multilayer architecture with a thickness of 250–500 μm and tissue-like cellular density was constructed [138] (Fig. 10(a)). Both parenchymal and non-parenchymal components were deposited in user-defined spatial positions. Furthermore, a 3D printed hepatic toxicity testing model for drug-induced liver injury (DILI) at the tissue level was developed [140]. The model maintained the expression and drug-induced enzyme activity of Cytochrome P450s over 28 d in culture. The dose–response of Trovafloxacin was tested in comparison with Levofloxacin, and the results indicated that this model is capable of modeling tissue-level DILI effectively [140]. Bhise and colleagues [18] developed a bioreactor containing bioprinted hepatic constructs with human HepG2/C3A spheroids encapsulated in GelMA hydrogel (Fig. 10(b)). The bioreactor could support a long-term culture of 3D human HepG2/C3A spheroids for drug toxicity assessment. The toxic response induced by treatment with 15 $\text{mmol}\cdot\text{L}^{-1}$ acetaminophen was found to be comparable to that of existing *in vitro* models [18]. In addition, a one-step fabrication process was proposed by Lee and Cho [19] for fabricating a liver-on-a-chip (Fig. 10(c)). The chip demonstrated low protein absorption; hence, accurate measurement of metabolic activities and drug responses could be achieved. DLP technology was employed in the construction of a liver-on-a-chip as well [26] (Fig. 10(d)). The researchers fabricated a 3D triculture platform that embedded hiPSC-derived hepatic progenitor cells (hiPSC-HPCs) with human umbilical vein endothelial

cells (hUVECs) and adipose-derived stem cells in a hexagonal architecture. DLP can achieve the highest resolution and highest constructing speed among all bioprinting strategies, and thus facilitates the rapid fabrication of chips and the construction of heterogeneous structures.

5.2. Heart-on-a-chip

A heart-on-a-chip is a potential option for the evaluation of the cardiovascular toxicity of drugs. Lind and colleagues [20] integrated soft strain gauge sensors within a cell-laden microarchitecture to detect the contraction of bioprinted cardiac tissues (Fig. 10(e)). The heart-on-a-chip device was printed using six functional bioinks. Electronic readouts of muscle contractile stresses were obtained noninvasively by means of embedded sensors in cell incubator environments. The dose-related drug responses of the printed structures were investigated, and contractile development was studied during the four-week maturation. Zhang et al. [83] constructed a heart-on-a-chip by directly printing endothelial cells with hydrogels and seeding cardiomyocytes onto the endothelial bed (Figs. 10(f, g)). An aligned myocardium capable of spontaneous and synchronous contraction was generated. A microfluidic bioreactor was designed to contain the organoid in order to perform the toxicity assessment. The dose-dependent responses of the cells were observed, thus demonstrating the feasibility of this platform for toxicity evaluation.

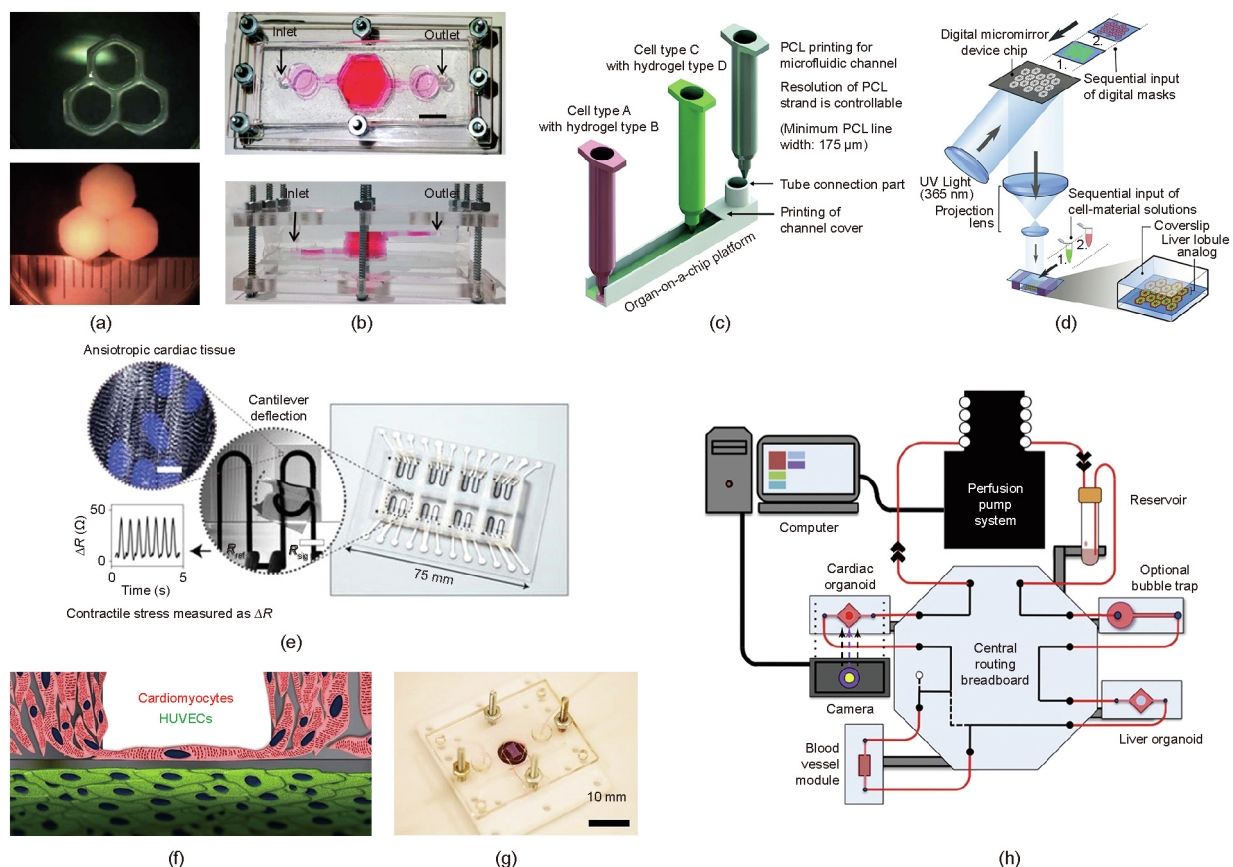


Fig. 10. 3D bioprinting of organs-on-chips. (a–d) Liver-on-a-chip: (a) A multilayer heterogeneous hepatic tissue with a thickness of 250–500 μm ; (b) a bioreactor containing a 3D bioprinted hepatic construct for the long-term culture of HepG2/C3A spheroids; (c) a one-step fabrication approach by multi-nozzle bioprinting for fabricating a liver-on-a-chip; (d) a DLP-fabricated 3D triculture model that embeds hiPSC-HPCs with hUVEC and adipose-derived stem cells in a microscale hexagonal architecture [26]. (e–g) Heart-on-a-chip: (e) A microphysiological device constructed by printing six functional bioinks and integrating soft strain gauge sensors for drug toxicity testing; (f, g) an organoid fabricated by seeding cardiomyocytes into an endothelialized hydrogel scaffold was embedded into a bioreactor for cardiovascular toxicity evaluation. (h) Schematic of a multi-organoid body-on-a-chip. (a) Reproduced from Ref. [138] with permission of Fedn of Am Societies for Experimental Bio, © 1987; (b) reproduced from Ref. [18] with permission of IOP Publishing, © 2009; (c) reproduced from Ref. [19] with permission of Royal Society of Chemistry, © 20116; (e) reproduced from Ref. [20] with permission of Springer Nature, © 2016; (f, g) reproduced from Ref. [83] with permission of Elsevier, © 2016; (h) reproduced from Ref. [137] with permission of Elsevier, © 2016.

Although studies have validated the capability of a heart-on-a-chip to evaluate drug-induced cardiovascular toxicity with versatility, further investigations are required to examine the underlying mechanisms of cell-drug interactions and intercellular activities. In addition, the role of cardiac cell alignment can be studied and the mechanism of force generation can be explored in order to better replicate that contractility and intercellular communication of native cardiac muscles. Several strategies have been proposed for measuring the contractile force generated by cardiomyocytes, including integrated strain sensors [141], micro-spring devices [123], and micro-cantilevers [142]. However, these strategies are only compatible with monolayer cardiac patches with aligned cardiomyocytes (CMs) or bulk cardiac tissue without aligning the embedded CMs. Therefore, an integrated heart-on-a-chip device is yet to be developed to tackle this issue.

5.3. Body-on-a-chip

In addition to the printing of liver-on-a-chips and heart-on-a-chips, other organs-on-chips including a lung-on-a-chip [8] and a kidney-on-a-chip [143] have been fabricated using non-printing approaches. A body-on-a-chip was recently reported as well [137], as shown in Fig. 10(h).

Huh and colleagues [8] were the first to propose the concept of a lung-on-a-chip. An alveolar-capillary barrier was constructed to mimic the organ-level functions of the human lung. The results of nanotoxicity studies indicated that the lung-on-a-chip reproduced the toxic and inflammatory responses of the lung. Using the same protocol, researchers developed a kidney-on-a-chip device that reconstituted the glomerular-capillary-wall function [143]. In this model, human-induced pluripotent stem (hiPS) cells differentiated into podocytes with the expression of mature phenotype markers (nephrin⁺, WT1⁺, podocin⁺, and PAX2⁺).

A body-on-a-chip platform integrates multiple functional organoids including a cardiac organoid, liver organoid, blood vessel module, and so forth, along with a microfluidic perfusion system [137]. This technology will significantly improve the efficiency and lower the cost of the drug-discovery pipeline. However, achieving high throughput and formulating suitable culture media are limitations to the application of the body-on-a-chip.

6. Challenges and perspective

Although 3D bioprinting technology has been widely employed in tissue engineering, disease studies, and drug screening, many issues are yet to be addressed. Table 4 lists the main challenges in bioprinting various tissues and organs [12,14,15,19,20,62,83,103–105,112,116,118,137,138,144]. Common challenges related to bioprinting strategies, bioinks, and vascularization are discussed in this section.

At present, none of the existing bioprinting technologies (IBP, EBP, or LBP) can completely meet the demands of building artificial

tissues or organs-on-chips due to the limitations of printing speed, resolution, or compatibility with biomaterials. Printing speed must be improved in order to fabricate implementable constructs at clinically relevant sizes. A continuous liquid interface (CLIP) approach has demonstrated the capability of fabricating constructs on the centimeter scale with a feature resolution below 100 μm in minutes instead of hours [145], and will likely be used for tissue/organ fabrication. Efforts to improve resolution must be made for depositing biomaterials, cells, or biomolecules with precisely controlled gradients. Recently, a melt electro-writing (MEW) technique was advanced for the generation and stacking of ultrafine filaments (10–20 μm , up to 50 layers) [146,147]. This technique combines the strengths of 3D printing and electrospinning and opens an avenue for high-resolution additive manufacturing. Moreover, multi-nozzle bioprinters [12,44,148] or hybrid printing strategies [96,115] are beneficial for incorporating various biomaterials and for manufacturing complex constructs with structural and functional heterogeneity. With these improvements and novel techniques, artificial transplantable tissues are likely to be fabricated in a short time with a fine microstructure and macrostructure as well as realistic functionalities.

The balance between processability and biocompatibility is the main challenge in the development of bioinks. This balance is commonly achieved by using easily processable, mechanically strong materials as the structural supports and biocompatible hydrogels as the ECM components. However, it requires a rapid shift between different printing modules. Ober's group [149] developed an active mixing system that could homogenize a range of fluids at the microscale, and is a potential tool for dynamically tuning the rheological properties of bioinks. A continuous multi-material extrusion approach provides another direction for a rapidly shifting platform by switching reservoirs rather than printing nozzles [84,150]. By adding the thermosensitive gelatin and dual crosslinking approach, Yin et al. [77] improved the fidelity of low-concentration GelMA to the level of high-concentration GelMA, while maintained higher cytocompatibility. To reduce cell damage during the printing process and improve the viability, visible light crosslinkable bioinks have been introduced [84,151]. Moreover, the microenvironments in the ECM of native tissues must be better understood in order to guide the construction of synthetic ECM with tissue-specific compositions and gradients [21]. Standardized characterization of bioinks for 3D bioprinting applications is needed, so that the performance of various bioinks can be better compared [152]. More importantly, the degradation of biomaterials should be emphasized. After being implemented *in vivo*, printed tissues should support the initial position of the embedded cells and degrade over time without generating toxic byproducts.

The incorporation of terminally differentiated cells and stem cells is a trend in 3D bioprinting. Multiple types of cells are essential for reproducing cell–cell interactions and recapitulating the functionality of tissues or organs. Research on the underlying mechanisms of stem cell proliferation and differentiation is particularly important. Studies have shown that stem cell fate

Table 4
Challenges in bioprinting tissues and organs.

Tissue/organ	Challenges	Refs.
Cartilage and bone	Gradient osteochondral constructs; integration with the host environment; mechanical strength; growth factor for improving functionality	[103–105]
Skin	Epidermis-dermis interface; vascularization; involve secondary and adnexal structures	[112,116,118]
Muscle	Pre-alignment of muscle cells; vascularization and innervation	[12,83]
Vasculature	Fabrication of functional multilayer vessel; 3D, hierarchical, and biomimicry vascular structure; integration with other tissues	[14,15,62]
Liver-on-a-chip	Native-like microenvironments; integrated fabrication approach	[19,138]
Heart-on-a-chip	Force measurement of multilayer, well-organized cardiac tissue; maturation and formation of cardiac tissues	[20,144]
Body-on-a-chip	Integration of different tissues; achievement of high throughput	[137]

can be directed by the specific spatiotemporal distribution of biomolecules [89]. The capability of precisely patterning cells and bioactive factors plays a vital role in the fabrication of artificial tissues or organs that can mimic their native counterparts. The cell-material interface may need to be studied further in order to obtain guidelines for selecting suitable materials for specific tissues. In addition, perfusable bioreactors should be designed to provide appropriate cellular environments with specific physical or chemical stimuli and to ensure cell viability and functioning.

Vascularization and innervation are common challenges in the field of tissue engineering [21], especially when constructing scale-up tissues or organs. Vascular networks in large-volume tissues are vital for providing passage to nutrients, oxygen, and metabolic wastes. Both complex perfusable vascular networks with hierarchical branches and large-diameter blood vessels have already been developed [125,128]. Recent advances have shown that the vascular network could support the long-term perfusion of a construct that exceeds 1 cm in thickness [14]. Lee et al. [40] developed a multiscale vascular network from millimeter-scale channels to micrometer-scale capillaries. Coaxial extrusion has been shown to be capable of fabricating a multiscale vessel-like structure with a diameter up to 8 mm [153]. Many studies have incorporated sacrificial materials within engineered tissues and subsequently removed them to form branched and perfusable channels [63,125]. However, a 3D, hierarchical, and biomimicry vascular network that can be integrated with host tissues has not yet been achieved and thus should be studied in future. Recently, Wang and colleagues [154] developed freestanding hierarchically branched structures using ice as a 3D printed sacrificial material. The structures were optimized to withstand surgical suturing, potentially enabling integration with the host vascular networks. Although the resolution of their platform was limited to 1 mm, these scholars opened an avenue for engineering vessel replacements and developing the next-generation vascular constructs [155]. Innervation is a further step toward constructing functioning tissues or organs [156], and is expected to enable the responses of tissues to their surroundings.

In summary, achievements in 3D bioprinting solid tissues and hollow tissues will interact with and promote each other, thus facilitating the construction of scale-up, functional, and transplantable tissues/organs that live longer. This development will offer a patient-specific and life-saving option for patients on organ transplantation waiting lists. Moreover, these high-performance tissues/organs—given progress in stem cell technology, bioreactors, microfluidic technology, and organ-on-a-chip devices—are expected to be more reliable, high-throughput, and cost-friendly. The mechanisms of diseases and the responses to drugs will be understood, bringing many future benefits to humanity.

7. Conclusions

This paper reviews recent advances in 3D bioprinting strategies and bioinks and in the application of 3D bioprinting technology in tissue engineering, disease studies, and drug screening. Printing speed, resolution, and compatibility with biomaterials require further improvement, and multi-channel printers will enable the engineering of more complex functional tissues and organs. Novel biomaterials with fine mechanical properties and high cytocompatibility will be beneficial in recapitulating extracellular environments. The combination of stem cell technology and 3D bioprinting is expected to allow the construction of better functioning tissues/organs and organs-on-chips. For the longevity and functionality of printed architectures, vascularization and innervation should be further investigated. Once these issues have been addressed, transplantable tissues/organs that are constructed *in vitro* and organs-on-chips that are capable of reproducing

organ-level responses will significantly promote the development of tissue engineering and regenerative medicine.

Acknowledgements

The authors would like to acknowledge support from the National Natural Science Foundation of China (51875518, 51475419, and 81501607), the Natural Science Foundation of Zhejiang Province of China (LY15H160019), and the Key Research and Development Projects of Zhejiang Province (2017C01054).

Compliance with ethics guidelines

Bin Zhang, Lei Gao, Liang Ma, Yichen Luo, Huayong Yang, and Zhanfeng Cui declare that they have no conflict of interest or financial conflicts to disclose.

References

- [1] Abouna GM. Organ shortage crisis: problems and possible solutions. *Transplant Proc* 2008;40(1):34–8.
- [2] Zhang B, Luo Y, Ma L, Gao L, Li Y, Xue Q, et al. 3D bioprinting: an emerging technology full of opportunities and challenges. *Bio-Des Manuf* 2018;1(1):2–13.
- [3] Ozbolat IT, Yu Y. Bioprinting toward organ fabrication: challenges and future trends. *IEEE Trans Biomed Eng* 2013;60(3):691–9.
- [4] An N, Shi Y, Jiang Y, Zhao L. Organ donation in China: the major progress and the continuing problem. *J Biomed Res* 2016;30(2):81–2.
- [5] Langer R, Vacanti JP. Tissue engineering. *Science* 1993;260(5110):920–6.
- [6] Oberpenning F, Meng J, Yoo JJ, Atala A. De novo reconstitution of a functional mammalian urinary bladder by tissue engineering. *Nat Biotechnol* 1999;17(2):149–55.
- [7] Jiang J, Yi HG, Cho DW. 3D printed tissue models: present and future. *ACS Biomater Sci Eng* 2016;2(10):1722–31.
- [8] Huh D, Matthews BD, Mammoto A, Montoya-Zavala M, Hsin HY, Ingber DE. Reconstituting organ-level lung functions on a chip. *Science* 2010;328(5986):1662–8.
- [9] Morimoto Y, Onoe H, Takeuchi S. Biohybrid robot powered by an antagonistic pair of skeletal muscle tissues. *Sci Rob* 2018;3(18):eaat4440.
- [10] Choi YJ, Kim TG, Jeong J, Yi HG, Park JW, Hwang W, et al. 3D cell printing of functional skeletal muscle constructs using skeletal muscle-derived bioink. *Adv Healthc Mater* 2016;5(20):2636–45.
- [11] Cubo N, Garcia M, Del Cañizo JF, Velasco D, Jorcano JL. 3D bioprinting of functional human skin: production and *in vivo* analysis. *Biofabrication* 2016;9(1):015006.
- [12] Kang HW, Lee SJ, Ko IK, Kengla C, Yoo JJ, Atala A. A 3D bioprinting system to produce human-scale tissue constructs with structural integrity. *Nat Biotechnol* 2016;34(3):312–9.
- [13] Dolati F, Yu Y, Zhang Y, Jesus AMD, Sander EA, Ozbolat IT. *In vitro* evaluation of carbon-nanotube-reinforced bioprintable vascular conduits. *Nanotechnology* 2014;25(14):145101.
- [14] Kolesky DB, Homan KA, Skylar-Scott MA, Lewis JA. Three-dimensional bioprinting of thick vascularized tissues. *Proc Natl Acad Sci USA* 2016;113(12):3179–84.
- [15] Norotte C, Marga FS, Niklason LE, Forgacs G. Scaffold-free vascular tissue engineering using bioprinting. *Biomaterials* 2009;30(30):5910–7.
- [16] Zhu W, Qu X, Zhu J, Ma X, Patel S, Liu J, et al. Direct 3D bioprinting of prevascularized tissue constructs with complex microarchitecture. *Biomaterials* 2017;124:106–15.
- [17] Fu F, Shang L, Chen Z, Yu Y, Zhao Y. Bioinspired living structural color hydrogels. *Sci Rob* 2018;3(16):eaar8580.
- [18] Bhise NS, Manoharan V, Massa S, Tamayol A, Ghaderi M, Miscuglio M, et al. A liver-on-a-chip platform with bioprinted hepatic spheroids. *Biofabrication* 2016;8(1):014101.
- [19] Lee H, Cho DW. One-step fabrication of an organ-on-a-chip with spatial heterogeneity using a 3D bioprinting technology. *Lab Chip* 2016;16(14):2618–25.
- [20] Lind JU, Busbee TA, Valentine AD, Pasqualini FS, Yuan H, Yadid M, et al. Instrumented cardiac microphysiological devices via multimaterial three-dimensional printing. *Nat Mater* 2017;16(3):303–8.
- [21] Barnatt C. Future visions: bioprinter [Internet]. ExplainingTheFuture.com; 2011 [cited 2017 Jun 6]. Available from: http://www.explainingthefuture.com/visions/vision_bioprinter.html.
- [22] Murphy SV, Atala A. 3D bioprinting of tissues and organs. *Nat Biotechnol* 2014;32(8):773–85.
- [23] Zhang YS, Yue K, Aleman J, Moghaddam KM, Bakht SM, Yang J, et al. 3D bioprinting for tissue and organ fabrication. *Ann Biomed Eng* 2017;45(1):148–63.
- [24] Gao G, Yonezawa T, Hubbell K, Dai G, Cui X. Inkjet-bioprinted acrylated peptides and PEG hydrogel with human mesenchymal stem cells promote

- robust bone and cartilage formation with minimal printhead clogging. *Biotechnol J* 2015;10(10):1568–77.
- [25] Skardal A, Mack D, Kapetanovic E, Atala A, Jackson JD, Yoo J, et al. Bioprinted amniotic fluid-derived stem cells accelerate healing of large skin wounds. *Stem Cells Transl Med* 2012;1(11):792–802.
- [26] Ma X, Qu X, Zhu W, Li YS, Yuan S, Zhang H, et al. Deterministically patterned biomimetic human iPSC-derived hepatic model via rapid 3D bioprinting. *Proc Natl Acad Sci USA* 2016;113(8):2206–11.
- [27] Guvendiren M, Molde J, Soares RMD, Kohn J. Designing biomaterials for 3D printing. *ACS Biomater Sci Eng* 2016;2(10):1679–93.
- [28] Soman P, Chung PH, Zhang AP, Chen S. Digital microfabrication of user-defined 3D microstructures in cell-laden hydrogels. *Biotechnol Bioeng* 2013;110(11):3038–47.
- [29] Obata K, El-Tamer A, Koch L, Hinze U, Chichkov BN. High-aspect 3D two-photon polymerization structuring with widened objective working range (WOW-2PP). *Light Sci Appl* 2013;2:e116.
- [30] Cui X, Breitenkamp K, Finn MG, Lotz M, D'Lima DD. Direct human cartilage repair using three-dimensional bioprinting technology. *Tissue Eng Part A* 2012;18(11–12):1304–12.
- [31] Lee VK, Kim DY, Ngo H, Lee Y, Seo L, Yoo SS, et al. Creating perfused functional vascular channels using 3D bio-printing technology. *Biomaterials* 2014;35(28):8092–102.
- [32] Jia W, Gungor-Ozkerim PS, Zhang YS, Yue K, Zhu K, Liu W, et al. Direct 3D bioprinting of perfusable vascular constructs using a blend bioink. *Biomaterials* 2016;106:58–68.
- [33] Michael S, Sorg H, Peck CT, Koch L, Deiwick A, Chichkov B, et al. Tissue engineered skin substitutes created by laser-assisted bioprinting form skin-like structures in the dorsal skin fold chamber in mice. *PLoS One* 2013;8(3):e57741.
- [34] Gao Q, He Y, Fu J, Qiu J, Jin Y. Fabrication of shape controllable alginate microparticles based on drop-on-demand jetting. *J Sol-Gel Sci Technol* 2016;77(3):610–9.
- [35] Cui X, Boland T. Human microvasculature fabrication using thermal inkjet printing technology. *Biomaterials* 2009;30(31):6221–7.
- [36] Wilson Jr WC, Boland T. Cell and organ printing 1: protein and cell printers. *Anat Rec A Discov Mol Cell Evol Biol* 2003;272A(2):491–6.
- [37] Xu T, Kincaid H, Atala A, Yoo JJ. High-throughput production of single-cell microparticles using an inkjet printing technology. *J Manuf Sci Eng* 2008;130(2):021017.
- [38] Wang Y, Li X, Li C, Yang M, Wei Q. Binder droplet impact mechanism on a hydroxyapatite microsphere surface in 3D printing of bone scaffolds. *J Mater Sci* 2015;50(14):5014–23.
- [39] Brunello G, Sivolella S, Meneghello R, Ferroni L, Gardin C, Piattelli A, et al. Powder-based 3D printing for bone tissue engineering. *Biotechnol Adv* 2016;34(5):740–53.
- [40] Lee VK, Lanzi AM, Ngo H, Yoo SS, Vincent PA, Dai G. Generation of multi-scale vascular network system within 3D hydrogel using 3D bio-printing technology. *Cell Mol Bioeng* 2014;7(3):460–72.
- [41] Mandrycky C, Wang Z, Kim K, Kim DH. 3D bioprinting for engineering complex tissues. *Biotechnol Adv* 2016;34(4):422–34.
- [42] Skardal A, Atala A. Biomaterials for integration with 3D bioprinting. *Ann Biomed Eng* 2015;43(3):730–46.
- [43] Merceron TK, Burt M, Seol YJ, Kang HW, Lee SJ, Yoo JJ, et al. A 3D bioprinted complex structure for engineering the muscle-tendon unit. *Biofabrication* 2015;7(3):035003.
- [44] Ozbolat IT, Chen H, Yu Y. Development of 'multi-arm bioprinter' for hybrid biofabrication of tissue engineering constructs. *Robot Comput Integr Manuf* 2014;30(3):295–304.
- [45] Gao Q, He Y, Fu JZ, Liu A, Ma L. Coaxial nozzle-assisted 3D bioprinting with built-in microchannels for nutrients delivery. *Biomaterials* 2015;61:203–15.
- [46] Yu Y, Moncal KK, Li J, Peng W, Rivero I, Martin JA, et al. Three-dimensional bioprinting using self-assembling scalable scaffold-free "tissue strands" as a new bioink. *Sci Rep* 2016;6(1):28714.
- [47] Daly AC, Critchley SE, Rencsok EM, Kelly DJ. A comparison of different bioinks for 3D bioprinting of fibrocartilage and hyaline cartilage. *Biofabrication* 2016;8(4):045002.
- [48] Kinstlinger IS, Miller JS. 3D-printed fluidic networks as vasculature for engineered tissue. *Lab Chip* 2016;16(11):2025–43.
- [49] Jian H, Wang M, Wang S, Wang A, Bai S. 3D bioprinting for cell culture and tissue fabrication. *Bio-Des Manuf* 2018;1(1):45–61.
- [50] Warner J, Soman P, Zhu W, Tom M, Chen S. Design and 3D printing of hydrogel scaffolds with fractal geometries. *ACS Biomater Sci Eng* 2016;2(10):1763–70.
- [51] Koch L, Deiwick A, Schlie S, Michael S, Gruene M, Coger V, et al. Skin tissue generation by laser cell printing. *Biotechnol Bioeng* 2012;109(7):1855–63.
- [52] Koch L, Brandt O, Deiwick A, Chichkov B. Laser assisted bioprinting at different wavelengths and pulse durations with a metal dynamic release layer: a parametric study. *Int J Bioprint* 2017;3(1).
- [53] Hribar KC, Soman P, Warner J, Chung P, Chen S. Light-assisted direct-write of 3D functional biomaterials. *Lab Chip* 2014;14(2):268–75.
- [54] Nguyen AK, Narayan RJ. Two-photon polymerization for biological applications. *Mater Today* 2017;20(6):314–22.
- [55] Mandt D, Gruber P, Markovic M, Tromayer M, Rothbauer M, Krayz SRA, et al. Fabrication of placental barrier structures within a microfluidic device utilizing two-photon polymerization. *Int J Bioprint* 2018;4(2).
- [56] Gao L, Kupfer ME, Jung JP, Yang L, Zhang P, Da Sie Y, et al. Myocardial tissue engineering with cells derived from human-induced pluripotent stem cells and a native-like, high-resolution, three-dimensionally printed scaffold. *Circ Res* 2017;120(8):1318–25.
- [57] Hospodiuk M, Dey M, Sosnoski D, Ozbolat IT. The bioink: a comprehensive review on bioprintable materials. *Biotechnol Adv* 2017;35(2):217–39.
- [58] Hsieh FY, Lin HH, Hsu SH. 3D bioprinting of neural stem cell-laden thermoresponsive biodegradable polyurethane hydrogel and potential in central nervous system repair. *Biomaterials* 2015;71:48–57.
- [59] Rhee S, Puetzer JL, Mason BN, Reinhart-King CA, Bonassar LJ. 3D bioprinting of spatially heterogeneous collagen constructs for cartilage tissue engineering. *ACS Biomater Sci Eng* 2016;2(10):1800–5.
- [60] Hung KC, Tseng CS, Dai LG, Hsu SH. Water-based polyurethane 3D printed scaffolds with controlled release function for customized cartilage tissue engineering. *Biomaterials* 2016;83:156–68.
- [61] Martínez Ávila H, Schwarz S, Rotter N, Gatenholm P. 3D bioprinting of human chondrocyte-laden nanocellulose hydrogels for patient-specific auricular cartilage regeneration. *Bioprinting* 2016;1–2:22–35.
- [62] Christensen K, Xu C, Chai W, Zhang Z, Fu J, Huang Y. Freeform inkjet printing of cellular structures with bifurcations. *Biotechnol Bioeng* 2015;112(5):1047–55.
- [63] Bertassoni LE, Cecconi M, Manoharan V, Nikkha M, Hjortnaes J, Cristino AL, et al. Hydrogel bioprinted microchannel networks for vascularization of tissue engineering constructs. *Lab Chip* 2014;14(13):2202–11.
- [64] Malafaya PB, Reis RL. Bilayered chitosan-based scaffolds for osteochondral tissue engineering: influence of hydroxyapatite on *in vitro* cytotoxicity and dynamic bioactivity studies in a specific double-chamber bioreactor. *Acta Biomater* 2009;5(2):644–60.
- [65] Ng WL, Yeong WY, Naing MW. Development of polyelectrolyte chitosan-gelatin hydrogels for skin bioprinting. *Procedia CIRP* 2016;49:105–12.
- [66] Lee JS, Hong JM, Jung JW, Shim JH, Oh JH, Cho DW. 3D printing of composite tissue with complex shape applied to ear regeneration. *Biofabrication* 2014;6(2):024103.
- [67] Kolesky DB, Truby RL, Gladman AS, Busbee TA, Homan KA, Lewis JA. 3D bioprinting of vascularized, heterogeneous cell-laden tissue constructs. *Adv Mater* 2014;26(19):3124–30.
- [68] Hung BP, Naved BA, Nyberg EL, Dias M, Holmes CA, Elisseeff JH, et al. Three-dimensional printing of bone extracellular matrix for craniofacial regeneration. *ACS Biomater Sci Eng* 2016;2(10):1806–16.
- [69] Duan B. State-of-the-art review of 3D bioprinting for cardiovascular tissue engineering. *Ann Biomed Eng* 2017;45(1):195–209.
- [70] Owens CM, Marga F, Forgacs G, Heesch CM. Biofabrication and testing of a fully cellular nerve graft. *Biofabrication* 2013;5(4):045007.
- [71] Ouyang L, Highley CB, Rodell CB, Sun W, Burdick JA. 3D Printing of shear-thinning hyaluronic acid hydrogels with secondary cross-linking. *ACS Biomater Sci Eng* 2016;2(10):1743–51.
- [72] Narayanan LK, Huebner P, Fisher MB, Spang JT, Starly B, Shirwaiker RA. 3D-bioprinting of polylactic acid (PLA) nanofiber-alginate hydrogel bioink containing human adipose-derived stem cells. *ACS Biomater Sci Eng* 2016;2(10):1732–42.
- [73] Jungst T, Smolan W, Schacht K, Scheibel T, Groll J. Strategies and molecular design criteria for 3D printable hydrogels. *Chem Rev* 2016;116(3):1496–539.
- [74] Faulkner-Jones A, Fyfe C, Cornelissen DJ, Gardner J, King J, Courtney A, et al. Bioprinting of human pluripotent stem cells and their directed differentiation into hepatocyte-like cells for the generation of mini-livers in 3D. *Biofabrication* 2015;7(4):044102.
- [75] Ying G, Jiang N, Yu C, Zhang YS. Three-dimensional bioprinting of gelatin methacryloyl (GelMA). *Bio-Des Manuf* 2018;1(4):215–24.
- [76] Gao G, Schilling AF, Hubbell K, Yonezawa T, Truong D, Hong Y, et al. Improved properties of bone and cartilage tissue from 3D inkjet-bioprinted human mesenchymal stem cells by simultaneous deposition and photocrosslinking in PEG-GelMA. *Biotechnol Lett* 2015;37(11):2349–55.
- [77] Yin J, Yan M, Wang Y, Fu J, Suo H. 3D bioprinting of low-concentration cell-laden gelatin methacrylate (GelMA) bioinks with a two-step cross-linking strategy. *ACS Appl Mater Interfaces* 2018;10(8):6849–57.
- [78] Massa S, Sakr MA, Seo J, Bandaru P, Arneri A, Bersini S, et al. Bioprinted 3D vascularized tissue model for drug toxicity analysis. *Biomed Microfluidics* 2017;11(4):044109.
- [79] Perniconi B, Costa A, Aulino P, Teodori L, Adamo S, Coletti D. The pro-myogenic environment provided by whole organ scale acellular scaffolds from skeletal muscle. *Biomaterials* 2011;32(31):7870–82.
- [80] Pati F, Jiang J, Ha DH, Won Kim S, Rhie JW, Shim JH, et al. Printing three-dimensional tissue analogues with decellularized extracellular matrix bioink. *Nat Commun* 2014;5(1):3935.
- [81] Gill EL, Li X, Birch MA, Huang YYS. Multi-length scale bioprinting towards simulating microenvironmental cues. *Biodes Manuf* 2018;1(2):77–88.
- [82] Wang Z, Abdulla R, Parker B, Samanipour R, Ghosh S, Kim K. A simple and high-resolution stereolithography-based 3D bioprinting system using visible light crosslinkable bioinks. *Biofabrication* 2015;7(4):045009.
- [83] Zhang YS, Arneri A, Bersini S, Shin SR, Zhu K, Goli-Malekabadi Z, et al. Bioprinting 3D microfibrous scaffolds for engineering endothelialized myocardium and heart-on-a-chip. *Biomaterials* 2016;110:45–59.
- [84] Ahadian S, Khademhosseini A. A perspective on 3D bioprinting in tissue regeneration. *Biodes Manuf* 2018;1(3):157–60.
- [85] Zhang Y. Post-3D printing modification for improved biomedical applications. *Int J Bioprint* 2017;3(2):93–9.

- [86] Jakab K, Neagu A, Mironov V, Markwald RR, Forgacs G. Engineering biological structures of prescribed shape using self-assembling multicellular systems. *Proc Natl Acad Sci USA* 2004;101(9):2864–9.
- [87] Thomson JA, Itskovitz-Eldor J, Shapiro SS, Waknitz MA, Swiergiel JJ, Marshall VS, et al. Embryonic stem cell lines derived from human blastocysts. *Science* 1998;282(5391):1145–7.
- [88] Mehrban N, Teoh GZ, Birchall MA. 3D bioprinting for tissue engineering: stem cells in hydrogels. *Int J Bioprint* 2016;2.
- [89] Tasoglu S, Demirci U. Bioprinting for stem cell research. *Trends Biotechnol* 2013;31(1):10–9.
- [90] Ouyang L, Yao R, Mao S, Chen X, Na J, Sun W. Three-dimensional bioprinting of embryonic stem cells directs highly uniform embryoid body formation. *Biofabrication* 2015;7(4):044101.
- [91] Knoepfler PS. Deconstructing stem cell tumorigenicity: a roadmap to safe regenerative medicine. *Stem Cells* 2009;27(5):1050–6.
- [92] Körbling M, Estrov Z, Champlin R. Adult stem cells and tissue repair. *Bone Marrow Transplant* 2003;32(S1):S23–4.
- [93] Du M, Chen B, Meng Q, Liu S, Zheng X, Zhang C, et al. 3D bioprinting of BMSC-laden methacrylamide gelatin scaffolds with CBD-BMP2-collagen microfibers. *Biofabrication* 2015;7(4):044104.
- [94] Ye K, Felimban R, Traianedes K, Moulton SE, Wallace GG, Chung J, et al. Chondrogenesis of infrapatellar fat pad derived adipose stem cells in 3D printed chitosan scaffold. *PLoS One* 2014;9(6):e99410.
- [95] Richardson SM, Kalamegam G, Pushparaj PN, Matta C, Memic A, Khademhosseini A, et al. Mesenchymal stem cells in regenerative medicine: focus on articular cartilage and intervertebral disc regeneration. *Methods* 2016;99:69–80.
- [96] Xu T, Binder KW, Albanna MZ, Dice D, Zhao W, Yoo JJ, et al. Hybrid printing of mechanically and biologically improved constructs for cartilage tissue engineering applications. *Biofabrication* 2013;5(1):015001.
- [97] Müller M, Öztürk E, Arlov Ø, Gatenholm P, Zenobi-Wong M. Alginate sulfate-nanocellulose bioinks for cartilage bioprinting applications. *Ann Biomed Eng* 2017;45(1):210–23.
- [98] Sawkins MJ, Mistry P, Brown BN, Shakesheff KM, Bonassar LJ, Yang J. Cell and protein compatible 3D bioprinting of mechanically strong constructs for bone repair. *Biofabrication* 2015;7(3):035004.
- [99] Abaci HE, Guo Z, Coffman A, Gillette B, Lee WH, Sia SK, et al. Human skin constructs with spatially controlled vasculature using primary and iPSC-derived endothelial cells. *Adv Healthc Mater* 2016;5(14):1800–7.
- [100] O'Connell G, Garcia J, Amir J. 3D bioprinting: new directions in articular cartilage tissue engineering. *ACS Biomater Sci Eng* 2017;3(11):2657–68.
- [101] Li X, Ding J, Wang J, Zhuang X, Chen X. Biomimetic biphasic scaffolds for osteochondral defect repair. *Regen Biomater* 2015;2(3):221–8.
- [102] Atesok K, Doral MN, Karlsson J, Egol KA, Jazrawi LM, Coelho PG, et al. Multilayer scaffolds in orthopaedic tissue engineering. *Knee Surg Sports Traumatol Arthrosc* 2016;24(7):2365–73.
- [103] Lopa S, Madry H. Bioinspired scaffolds for osteochondral regeneration. *Tissue Eng Part A* 2014;20(15–16):2052–76.
- [104] Markstedt K, Mantas A, Tournier I, Martínez Ávila H, Hägg D, Gatenholm P. 3D bioprinting human chondrocytes with nanocellulose-alginate bioink for cartilage tissue engineering applications. *Biomacromolecules* 2015;16(5):1489–96.
- [105] Lv J, Xiu P, Tan J, Jia Z, Cai H, Liu Z. Enhanced angiogenesis and osteogenesis in critical bone defects by the controlled release of BMP-2 and VEGF: implantation of electron beam melting-fabricated porous Ti6Al4V scaffolds incorporating growth factor-doped fibrin glue. *Biomater* 2015;10(3):035013.
- [106] Monzón M, Liu C, Ajami S, Oliveira M, Donate R, Ribeiro V, et al. Functionally graded additive manufacturing to achieve functionality specifications of osteochondral scaffolds. *Bio-Des Manuf* 2018;1(1):69–75.
- [107] Schon BS, Hooper GJ, Woodfield TBF. Modular tissue assembly strategies for biofabrication of engineered cartilage. *Ann Biomed Eng* 2017;45(1):100–14.
- [108] Nukavarapu SP, Dorcemes DL. Osteochondral tissue engineering: current strategies and challenges. *Biotechnol Adv* 2013;31(5):706–21.
- [109] Vijayavenkataraman S, Lu WF, Fuh JYH. 3D bioprinting of skin: a state-of-the-art review on modelling, materials, and processes. *Biofabrication* 2016;8(3):032001.
- [110] Ng WL, Wang S, Yeong WY, Naing MW. Skin bioprinting: impending reality or fantasy? *Trends Biotechnol* 2016;34(9):689–99.
- [111] Lee W, Debasitis JC, Lee VK, Lee JH, Fischer K, Edminster K, et al. Multi-layered culture of human skin fibroblasts and keratinocytes through three-dimensional freeform fabrication. *Biomaterials* 2009;30(8):1587–95.
- [112] Lee V, Singh G, Trasatti JP, Björnsson C, Xu X, Tran TN, et al. Design and fabrication of human skin by three-dimensional bioprinting. *Tissue Eng Part C Methods* 2014;20(6):473–84.
- [113] Kim G, Ahn S, Yoon H, Kim Y, Chun W. A cryogenic direct-plotting system for fabrication of 3D collagen scaffolds for tissue engineering. *J Mater Chem* 2009;19(46):8817–23.
- [114] Kim G, Ahn S, Kim Y, Cho Y, Chun W. Coaxial structured collagen–alginate scaffolds: fabrication, physical properties, and biomedical application for skin tissue regeneration. *J Mater Chem* 2011;21(17):6165–72.
- [115] Kim BS, Lee JS, Gao G, Cho DW. Direct 3D cell-printing of human skin with functional transwell system. *Biofabrication* 2017;9(2):025034.
- [116] Kim BS, Kwon YW, Kong JS, Park GT, Gao G, Han W, et al. 3D cell printing of *in vitro* stabilized skin model and *in vivo* pre-vascularized skin patch using tissue-specific extracellular matrix bioink: a step towards advanced skin tissue engineering. *Biomaterials* 2018;168:38–53.
- [117] Ng WL, Qi JTZ, Yeong WY, Naing MW. Proof-of-concept: 3D bioprinting of pigmented human skin constructs. *Biofabrication* 2018;10(2):025005.
- [118] Min D, Lee W, Bae IH, Lee TR, Croce P, Yoo SS. Bioprinting of biomimetic skin containing melanocytes. *Exp Dermatol* 2018;27(5):453–9.
- [119] Cvetkovic C, Raman R, Chan V, Williams BJ, Tolish M, Bajaj P, et al. Three-dimensionally printed biological machines powered by skeletal muscle. *Proc Natl Acad Sci USA* 2014;111(28):10125–30.
- [120] Jiang W, Ma L, Xu X. Recent progress on the design and fabrication of micromotors and their biomedical applications. *Bio-Des Manuf* 2018;1(4):225–36.
- [121] Zhang J, Zhu W, Radisic M, Vunjak-Novakovic G. Can we engineer a human cardiac patch for therapy? *Circ Res* 2018;123(2):244–65.
- [122] Tijore A, Irvine SA, Sarig U, Mhaissalkar P, Baisane V, Venkatraman S. Contact guidance for cardiac tissue engineering using 3D printed gelatin patterned hydrogel. *Biofabrication* 2018;10(2):025003.
- [123] Wang Z, Lee SJ, Cheng HJ, Yoo JJ, Atala A. 3D bioprinted functional and contractile cardiac tissue constructs. *Acta Biomater* 2018;70:48–56.
- [124] Kucukgul C, Ozler SB, Inci I, Karakas E, Irmak S, Gozuacik D, et al. 3D bioprinting of biomimetic aortic vascular constructs with self-supporting cells. *Biotechnol Bioeng* 2015;112(4):811–21.
- [125] Miller JS, Stevens KR, Yang MT, Baker BM, Nguyen DHT, Cohen DM, et al. Rapid casting of patterned vascular networks for perfusable engineered three-dimensional tissues. *Nat Mater* 2012;11(9):768–74.
- [126] Neiman JAS, Raman R, Chan V, Rhoads MG, Raredon MSB, Velazquez JJ, et al. Photopatterning of hydrogel scaffolds coupled to filter materials using stereolithography for perfused 3D culture of hepatocytes. *Biotechnol Bioeng* 2015;112(4):777–87.
- [127] Nguyen DHT, Stapleton SC, Yang MT, Cha SS, Choi CK, Galie PA, et al. Biomimetic model to reconstitute angiogenic sprouting morphogenesis *in vitro*. *Proc Natl Acad Sci USA* 2013;110(17):6712–7.
- [128] Bhattacharjee T, Zehnder SM, Rowe KG, Jain S, Nixon RM, Sawyer WG, et al. Writing in the granular gel medium. *Sci Adv* 2015;1(8):e1500655.
- [129] Zhang Y, Yu Y, Akkouch A, Dababneh A, Dolati F, Ozbolat IT. *In vitro* study of directly bioprinted perfusable vasculature conduits. *Biomater Sci* 2015;3(1):134–43.
- [130] Mironov V, Visconti RP, Kasyanov V, Forgacs G, Drake CJ, Markwald RR. Organ printing: tissue spheroids as building blocks. *Biomaterials* 2009;30(12):2164–7.
- [131] Kucukgul C, Ozler B, Karakas HE, Gozuacik D, Koc B. 3D hybrid bioprinting of macrovascular structures. *Procedia Eng* 2013;59:183–92.
- [132] Jain RK, Au P, Tam J, Duda DG, Fukumura D. Engineering vascularized tissue. *Nat Biotechnol* 2005;23(7):821–3.
- [133] Suntornnond R, Tan EYS, An J, Chua CK. A highly printable and biocompatible hydrogel composite for direct printing of soft and perfusable vasculature-like structures. *Sci Rep* 2017;7(1):16902.
- [134] Duan B, Hockaday LA, Kang KH, Butcher JT. 3D bioprinting of heterogeneous aortic valve conduits with alginate/gelatin hydrogels. *J Biomed Mater Res A* 2013;101A(5):1255–64.
- [135] Duan B, Kapetanovic E, Hockaday LA, Butcher JT. Three-dimensional printed trileaflet valve conduits using biological hydrogels and human valve interstitial cells. *Acta Biomater* 2014;10(5):1836–46.
- [136] Peng W, Datta P, Ayan B, Ozbolat V, Sosnoski D, Ozbolat IT. 3D bioprinting for drug discovery and development in pharmaceuticals. *Acta Biomater* 2017;57:26–46.
- [137] Skardal A, Shupe T, Atala A. Organoid-on-a-chip and body-on-a-chip systems for drug screening and disease modeling. *Drug Discov Today* 2016;21(9):1399–411.
- [138] Robbins JB, Gorgen V, Min P, Shepherd BR, Presnell SC. A novel *in vitro* three-dimensional bioprinted liver tissue system for drug development. *FASEB J* 2013;27(872):12.
- [139] Nguyen D, Robbins J, Crogan-Grundy C, Gorgen V, Bangalore P, Perusse D, et al. Functional characterization of three-dimensional (3D) human liver tissues generated by an automated bioprinting platform. *FASEB J* 2015;29:LB424.
- [140] Nguyen DG, Funk J, Robbins JB, Crogan-Grundy C, Presnell SC, Singer T, et al. Bioprinted 3D primary liver tissues allow assessment of organ-level response to clinical drug induced toxicity *in vitro*. *PLoS One* 2016;11(7):e0158674.
- [141] Lind JU, Yadiid M, Perkins I, O'Connor BB, Eweje F, Chantre CO, et al. Cardiac microphysiological devices with flexible thin-film sensors for higher-throughput drug screening. *Lab Chip* 2017;17(21):3692–703.
- [142] Lai BFL, Huyer LD, Lu RXZ, Drecun S, Radisic M, Zhang B. InVADE: integrated vasculature for assessing dynamic events. *Adv Funct Mater* 2017;27(46):1703524.
- [143] Musah S, Mammoto A, Ferrante TC, Jeanty SSF, Hirano-Kobayashi M, Mammoto T, et al. Mature induced-pluripotent-stem-cell-derived human podocytes reconstitute kidney glomerular-capillary-wall function on a chip. *Nat Biomed Eng* 2017;1:0069.
- [144] Fleischer S, Shapira A, Feiner R, Dvir T. Modular assembly of thick multifunctional cardiac patches. *Proc Natl Acad Sci USA* 2017;114(8):1898–903.
- [145] Tumbleston JR, Shirvanyants D, Ermoshkin N, Januszewicz R, Johnson AR, Kelly D, et al. Continuous liquid interface production of 3D objects. *Science* 2015;347(6228):1349–52.

- [146] Hochleitner G, Fürsattel E, Giesa R, Groll J, Schmidt HW, Dalton PD. Melt electrowriting of thermoplastic elastomers. *Macromol Rapid Commun* 2018;39(10):e1800055.
- [147] Hrynevich A, Elçi BŞ, Haigh JN, McMaster R, Youssef A, Blum C, et al. Dimension-based design of melt electrowritten scaffolds. *Small* 2018;14(22):e1800232.
- [148] Shim JH, Lee JS, Kim JY, Cho DW. Bioprinting of a mechanically enhanced three-dimensional dual cell-laden construct for osteochondral tissue engineering using a multi-head tissue/organ building system. *J Micromech Microeng* 2012;22(8):085014.
- [149] Ober TJ, Foresti D, Lewis JA. Active mixing of complex fluids at the microscale. *Proc Natl Acad Sci USA* 2015;112(40):12293–8.
- [150] Liu W, Zhang YS, Heinrich MA, De Ferrari F, Jang HL, Bakht SM, et al. Rapid continuous multimaterial extrusion bioprinting. *Adv Mater* 2017;29(3):1604630.
- [151] Petta D, Armiento AR, Grijpma D, Alini M, Eglin D, D'Este M. 3D bioprinting of a hyaluronan bioink through enzymatic-and visible light-crosslinking. *Biofabrication* 2018;10(4):044104.
- [152] Townsend JM, Beck EC, Gehrke SH, Berkland CJ, Detamore MS. Flow behavior prior to crosslinking: the need for precursor rheology for placement of hydrogels in medical applications and for 3D bioprinting. *Prog Polym Sci* 2019;91:126–40.
- [153] Gao Q, Liu Z, Lin Z, Qiu J, Liu Y, Liu A, et al. 3D bioprinting of vessel-like structures with multilevel fluidic channels. *ACS Biomater Sci Eng* 2017;3(3):399–408.
- [154] Wang R, Ozsvar J, Aghaei-Ghareh-Bolagh B, Hiob MA, Mithieux SM, Weiss AS. Freestanding hierarchical vascular structures engineered from ice. *Biomaterials* 2019;192:334–45.
- [155] Yeo GC. A new vascular engineering strategy using 3D printed ice. *Trends Biotechnol* 2019;37(5):451–3.
- [156] Ozbolat IT, Peng W, Ozbolat V. Application areas of 3D bioprinting. *Drug Discov Today* 2016;21(8):1257–71.